Dissecting cell-specific functions of circadian genes using modified cell-specific CRISPR approaches

Shlesha Richhariya[1], Daniel Shin[1], Jasmine Quynh Le[1] and Michael Rosbash[1*]

Howard Hughes Medical Institute, Brandeis University, Waltham, MA 02454

*Correspondence – rosbash@brandeis.edu

Abstract

Circadian behavioral rhythms in *Drosophila melanogaster* are regulated by about 75 pairs of brain neurons. They all express the core clock genes but have distinct functions and gene expression profiles. To understand the importance of these distinct molecular programs, neuron-specific gene manipulations are essential. Although RNAi based methods are standard to manipulate gene expression in a cell-specific manner, they are often ineffective, especially in assays involving smaller numbers of neurons or weaker Gal4 drivers. We and others recently exploited a neuron-specific CRISPR-based method to mutagenize genes within circadian neurons. Here we further explore this approach to mutagenize three well-studied clock genes: the transcription factor gene *vrille*, the photoreceptor gene *Cryptochrome* (*cry*) and the neuropeptide gene *Pdf*. The CRISPR-based strategy not only reproduced their known phenotypes but also assigned a function for *cry* to two discrete subsets of clock neurons, a small subset of all *cry*-expressing cells. We further tested two recently published methods for temporal regulation in adult neurons, inducible Cas9 and auxin-inducible gene expression system (AGES). The results were not identical, but both approaches successfully showed that the adult-specific knockout of the neuropeptide *Pdf* reproduces the canonical loss-of-function mutant phenotypes. In summary, a CRISPR-based strategy is a highly effective, reliable, and general method to temporally manipulate gene function in specific adult neurons.

Introduction

Organismal behavior involves sensing the environment, internal processing, and motor actions. In multicellular organisms, this process is regulated largely by cells of the nervous system which often have defined roles as parts of bigger networks and circuits. One behavior that is almost ubiquitous to organisms on earth is aligning activity bouts to the daily rotations of the earth. The underlying mechanism is circadian rhythmicity.

In *Drosophila*, circadian clocks tick away in about 75 pairs of central brain clock neurons. These neurons all express the core circadian machinery, which includes the transcription factors CLOCK/CYCLE and the circadian inhibitory proteins PER/TIM. Rhythmic expression of these genes is important for maintaining circadian rhythmicity, and together they form a core transcription-translation feedback loop whose activity can be entrained by environmental cues such as light (Allada and Chung, 2010; Hardin, 2011; Helfrich-Förster, 2003). Clock neurons also express several accessory clock proteins, such as the transcription factors VRILLE (VRI) and PDP1; their losses result in more modest circadian phenotypes than the loss of core clock components (Blau & Young, 1999; Cyran et al., 2003).

Many additional genes are specifically expressed within clock neurons and also contribute to rhythmic behavior. Pigment dispersing factor (*Pdf*) encodes a circadian neuropeptide expressed exclusively within the small and large LNvs; *Pdf* mutants are arrhythmic and show increased sleep (Parisky et al., 2008; Renn et al., 1999). Another gene expressed by roughly half the clock neurons coding for the photoreceptor cryptochrome is *cry* (Benito et al., 2008; Emery et al., 1998; Stanewsky et al., 1998). Wild-type flies are arrhythmic in constant light, whereas *cry* mutants are rhythmic in this condition (Patrick Emery et al., 2000). Despite the specificity in expression and

probably function, few studies have explored the cell-type specific functions of these genes (Shafer and Taghert, 2009), and the cellular focus of many of circadian genes remains unknown.

Functional roles of specific circadian neurons have been broadly associated with the 7-8 subgroups based on anatomical location. For example, the PDF positive small LNvs are key regulators of rhythmicity under constant darkness and regulate morning activity. Another group of neurons, the 6 LNds along with the 5th sLNv, regulate evening activity and thus were labelled evening cells (Grima et al., 2004; Stoleru et al., 2004; Yao and Shafer, 2014; Dubowy and Sehgal, 2017). Yet other clock neuron subgroups play accessory roles in regulating rhythmicity and even sleep. They include the PDF-positive large LNvs, the DN1s, the DN2s, the LPNs and the mysterious DN3s (Shang et al., 2008; Zhang et al., 2010; Guo et al., 2016, 2018; King and Sehgal, 2020)

Recent single cell sequencing indicates at least 17 distinct subgroups, about twice as many as originally identified based on anatomical location (Ma et al., 2021). It is likely that many of these new subgroups are also functionally distinct. Fortunately, many of them can now be accessed through judicious use of the Gal4/UAS system (Brand and Perrimon, 1993; Luan et al., 2006), which allows for cell-type specific perturbations. This is because there are multiple Gal4 and split Gal4 drivers available to access specific circadian neurons (Meissner et al., 2022; Sekiguchi et al., 2020).

These drivers can be combined with the standard method of UAS-RNA interference (RNAi) to knockdown gene expression. Although this approach works well in many cases and has been invaluable for cell-type specific perturbations, it is often variable and usually induces partial knockdown (Dietzl et al., 2007; Meltzer et al., 2019). Fortunately, it is now possible to disrupt genes completely and in the same cell-specific manner using CRISPR/Cas9-based gene editing

(Port et al., 2014; Port and Boutros, 2022). Cas9 is an enzyme that induces a double stranded break at a specific genomic location determined by the guideRNA (gRNA) sequence (Jinek et al., 2012). The error prone repair machinery endogenous to all cells usually leads to mutations known as indels (insertions-deletions). These range from a missense mutation to a small addition or deletion causing frameshift mutations, often disrupting protein function (Port and Boutros, 2022).

Earlier adaptations of this method achieved cell specificity by expressing the Cas9 protein in a Gal4 dependent manner while ubiquitously expressing a single guide RNA against a gene of interest. The method was found to be more consistent and effective than RNAi in inducing loss of function phenotypes (Meltzer et al., 2019; Port et al., 2020). More recent developments such as multiplexing guides against a gene in an array under UAS control further improved both the efficiency and cell-type specificity (Port et al., 2020; Port and Bullock, 2016). This improved method worked well for disrupting the functions of the core clock genes *period* (*per*) and *timeless* (*tim*) in circadian neurons (Delventhal et al., 2019; Schlichting et al., 2019) and it was more recently extended to the disruption of genes encoding G-protein coupled receptors in these neurons (Schlichting et al., 2022).

Here, we implement this method to further understand the roles of three circadian behavior-associated genes: *vri, cry* and *Pdf*. We chose *vri* because there are no successful RNAi data in the literature, and we chose *cry* and *Pdf* to address precise cell-type specific function. Lastly, the CRISPR/Cas9 strategy was combined with two recent methods for temporal regulation, which successfully restricted gene editing and the resulting phenotype to specific neurons in just the adult stage. The results taken together substantially add to previous circadian analyses and identify specific subsets of clock neurons within which these genes function to regulate behavior.

Results

CRISPR mediated loss of VRI from clock neurons leads to a short circadian period.

Circadian behavioral rhythms are primarily regulated by a molecular program operating in clock neurons. One component of this program is the transcription factor VRI encoded by the essential gene *vrille (vri)*. Homozygous mutants are developmentally lethal (George and Terracol, 1997), and hemizygous mutants are strongly rhythmic but with a shorter free-running circadian period (Blau and Young, 1999). Cycling of VRI in clock neurons is likely important as constant over-expression in clock-expressing cells causes arrhythmicity and a longer circadian period (Blau and Young, 1999). However, an RNAi against *vri* in clock neurons did not affect circadian behavior (Matsumoto et al., 2007). We therefore developed a line with three CRISPR/Cas9 based 3X-guide-RNAs targeting the *vri* gene under UAS-control (*UAS-vri-g*). When expressed along with the reduced expression *UAS-Cas9.P2* (Meltzer et al., 2019) in clock neurons and the *CLK856-Gal4* driver, there was potent cell-type specific loss of VRI-staining (Fig. 1A, B, S1A). Importantly, the effect was shown to be specific as only VRI levels in Gal4-labeled cells were impacted; VRI levels in the DN3 neurons were unaffected (Fig. S1A) as expected since most of them are not labeled by the *CLK856-Gal4* driver (Ma et al., 2021). These flies had normal LD behavior but with a small evening peak advance compared to the control strains (Fig. S1B, C). Consistent with this phenotype, the flies were completely rhythmic in DD but with a significantly shorter circadian period (Fig. 1C-G). These phenotypes are identical to those of a recent *vri* mutant (Gunawardhana et al., 2021) indicating that they derive from the clock neurons.

CRY functions independently in two subsets of clock neurons

We next addressed the circadian gene *cry*, which encodes the photoreceptor Cryptochrome (CRY). Wild type flies are arrhythmic under constant bright light conditions, *cry* mutants in contrast remain rhythmic in constant light (Patrick Emery et al., 2000). This classic phenotype is reproduced when *cry* was mutated with *UAS-Cas9.P2* and *UAS-3X-cry-g* specifically in clock neurons using the *CLK856-Gal4* driver. Whereas only about 10 percent of the control flies were rhythmic in constant light (Rhythmicity Index>0.25), 90 percent of the *cry*-mutated flies were rhythmic (Fig. 2A-C, G, Table 1). These flies were also rhythmic in constant darkness, like the controls (Fig. S2) and like traditional *cry* mutants (Patrick Emery et al., 2000).

As *CLK856-Gal4* is expressed in most clock neurons, we then asked if the constant light phenotype could be assigned to a more specific subset of circadian neurons. All PDF neurons are CRY-positive (Benito et al., 2008; P. Emery et al., 2000), but disrupting *cry* in PDF cells with the *Pdf-Gal4* (Renn et al., 1999) had only a very small effect on constant light arrhythmicity (Fig. 2D, G, Table 1). In contrast, flies in which *cry* was mutated in the cells marked by the *dvPdf-Gal4* were fully rhythmic, indistinguishable from CRY loss in all circadian neurons (Fig. 2G, Table 1). This is interesting because the *dvPdf-Gal4* labels only 5 more cells per hemibrain than *Pdf-Gal4*, and only 2 of these 5 cells are CRY-positive: the 5th sLNv and the one ITP-positive LNd (Bahn et al., 2009; Schubert et al., 2018).

Ongoing work in the lab has characterized two Janelia split-Gal4 drivers, *ss00639-GAL4* and *ss00773-Gal4*. They both specifically label these two neurons in addition to very few additional (ectopic) cells (Le et. al., unpublished/in prep). Expression of CRISPR reagents against *cry* with the *ss00639-Gal4* driver also caused complete rhythmicity in constant light; more than 90% of the flies were rhythmic (Fig. 2E, G, Table 1). Similar but less strong results were seen with

ss00773-Gal4 (Fig 2G, Table 1). A third Gal4 driver, *MB122B-Gal4*, also expresses in these same two cells along with two additional LNd cells (Bulthuis et al., 2019; Guo et al., 2017), and mutating *cry* in cells labelled by this driver resulted in about 80% rhythmic flies in constant light (Fig. 2G, Table 1).

In addition to the lateral cells, CRY is expressed in the DN1p neurons labeled by the *CLK4.1-Gal4* driver (Zhang et al., 2010). Mutating *cry* in cells labeled by this driver also resulted in potent rhythmicity; nearly 75% of these flies were rhythmic in constant light (Fig. 2F, G, Table 1). These data taken together identify two sets of circadian neurons that can regulate rhythmicity independently under constant light in absence of CRY: two evening cells consisting of the 5th sLNv and the single ITP-positive LNd as well as the DN1p neurons.

To address possible mechanisms underlying the different groups of clock neurons and their regulation of constant light rhythmicity, we examined the circadian period of all rhythmic genotypes. Interestingly, *cry* mutants in all clock neurons have a circadian period of 24.7±0.7h in constant light, about an hour longer than their constant darkness period of 23.6±0.08 h (Fig. 2H, S2E). Mutating CRY in the evening cells with any of the 3 Gal4s gave rise to a similar period length of greater than 24 h, ~25h (Table 1, green boxes in Fig. 2H). Surprisingly, mutating CRY only in the DN1ps caused a dramatically shorter constant light period of ~22h (Table 1, Fig. 2H). These data indicate that there are interesting differences between these two discrete sets of circadian neurons (See Discussion).

PDF regulates activity and sleep from both the large and small LNvs.

A key circadian molecule beyond the core clock is the neuropeptide pigment dispersing factor (PDF); it is encoded by the gene *Pdf*. Null mutants of the gene (Pdf^{01}) are largely arrhythmic in

constant darkness (Renn et al., 1999). PDF is expressed in only 8 pairs of lateral neurons in the adult brain, four small (sLNvs) and four large (lLNvs) ventral lateral neurons per hemibrain. The lLNvs express very high levels of PDF, which can be easily visualized within their long arborizations. They extend to the optic lobes and to the other side of the brain. The sLNvs extend a long dorsal process, which is also marked by PDF staining (Fig. S3A, (Helfrich-Förster, 1997)).

A UAS-3X-gRNA line against *Pdf* (*UAS-Pdf-g*) in combination with the *Pdf-Gal4* driver that labels all PDF-producing neurons caused loss of PDF from the cell bodies and projections of most PDF neurons (Fig. 3A, B and S2B). There was however residual PDF staining in some lLNvs (Fig 3A, bottom panel, S2B), which likely reflects some residual PDF due to its very high levels in these cells prior to the mutagenesis. Nonetheless, this strain was completely arrhythmic in constant darkness whereas the parental control strains had normal rhythms (Fig. S4A-C, F).

We then used previously described split-Gal4 lines generated by the Rubin lab at Janelia (Schlichting et al., 2019) to specifically target only sLNvs or only lLNvs. The CRISPR/Cas9-based method was again highly effective in targeting PDF levels only in the cells targeted by the respective Gal4s. Expression of the gRNA and Cas9 in sLNv-specific driver (*ss00681-Gal4*) led to loss of PDF staining from 100% of the sLNvs examined and their dorsal processes, with no effect on the lLNv cell bodies or on their processes. Similarly, expressing the CRISPR reagents using the lLNv-specific driver (*ss00645-Gal4*) significantly reduced PDF expression from lLNv cell bodies and processes, without affecting PDF levels in the sLNvs or their dorsal process (Fig. 3A, B; S3B). However, the effect on the lLNvs was not as strong as about 20% of the neurons (1-2 neurons from about half the hemibrains) still had considerable PDF staining. This is not unlike the results with *Pdf-Gal4* (Fig. 3A, B-bottom panel) and probably due to the higher levels of PDF in the lLNvs (see Discussion). As expected based on earlier studies (Shafer and Taghert, 2009),

loss of PDF from small cells but not the large cells caused arrhythmicity in constant darkness (Fig. S4D-H).

Loss of PDF from both small and large PDF neurons caused increased sleep under constant darkness (Fig. 3C, F), and targeting the guides specifically to the small cells caused a similar sleep increase (Fig. 3D, G). This increase in sleep is not because of a lack of the ability to move as these flies are even more active than the controls when awake (Table 2). Although a role for PDF neurons in sleep and arousal has been described (Parisky et al., 2008; Sheeba et al., 2008), CRISPR-mediated loss of PDF specifically from the sLNvs here is the most direct evidence that the sLNvs regulate sleep. Loss of PDF from only the large cells also increased sleep but to a much smaller extent (Fig. 3E, H). Although the difference between the small and large cells may be due to the residual large cell PDF that escapes knockdown, the very significant reduction in PDF signal from lLNv cell bodies and processes makes it more likely that the lLNvs have a smaller role in regulating sleep under constant darkness.

An analysis of sleep structure indicated a substantial decrease in p-wake (the instantaneous probability that the flies will awaken from sleep), but no effect on p-doze (the instantaneous probability that awake flies will fall asleep) (Fig. 3H-J, Table 2). These data are consistent with a wake-promoting role of PDF (Parisky et al., 2008) and identify PDF from the sLNvs as the primary regulator.

Temporally regulated CRISPR/Cas9 mutagenesis assigns PDF function to adult neurons. The function of several circadian genes has not yet been definitively assigned to the adult fly, so some of them might have a substantial developmental role. Traditional methods of temporal regulation of Gal4 activity such as GeneSwitch (Osterwalder et al., 2001) or the temperature-

sensitive Gal80 system (McGuire et al., 2004) are not ideal for behavior experiments as they either involve toxic drugs or dramatic shifts in temperature, both of which severely impact the standard locomotor behavior assay (Li and Stavropoulos, 2016; Parisky et al., 2016). Pairing the temperature sensitive Gal80 system also resulted in leaky mutagenesis (Port et al., 2020). We therefore assessed two more recently developed methods, one specific to CRISPR and the other more general, to mutagenize adult-specifically genes of interest.

The first was the inducible Cas9 method developed by Port et. al. (Port et al., 2020). It is a UAS-based method: the Cas9 sequence is preceded by a GFP cassette, which is followed by a STOP codon flanked by FRT sites (hereafter called STOP-Cas9). Pairing with a heat-shock induced flp transgene allows for temporal control of mutagenesis as Cas9 expression occurs only post heat shock (Fig. S5A). We adapted this method for adult specific induction by using three consecutive heat shocks (referred to below as "heat shock"; see Methods). This STOP-Cas9 transgene was combined with *Pdf-Gal4*, *UAS-Pdf-g*, a *UAS-mRFP* transgene to label the PDF cells as well as a heat shock induced flp encoding hsFLPG5 (Fig. S5A).

In control flies without *UAS-Pdf-g*, heat shock did not affect either the levels of PDF (Fig. 4A, B, S5B) or rhythmic behavior (Fig. 4C, D). Importantly, flies expressing all the transgenes including the UAS-gRNA but without heat shock showed no loss of PDF signal (Fig. 4A, B, S5B) and no defects in behavior (Fig. 4C-F); this indicates no leaky expression without heat shock. In the same flies two weeks post heat shock, PDF staining was lost from all sLNvs in ~60% of the hemibrains analyzed, whereas some mosaicism was observed in the remaining 40% of the hemibrains; 1-2 neurons still expressed both GFP and PDF (Fig. 4A, B, S5B). A similar fraction of the heat shocked mutant flies, about 38 percent, were rhythmic in constant darkness (Fig. 4D,

S5C), indicating an adult-specific requirement of PDF for rhythmicity. The ca. 60 percent arrhythmic flies also showed an adult specific effect of PDF on sleep (Fig. 4E).

The remaining rhythmic flies likely reflect mosaicism, as PDF from 1-2 neurons might be sufficient to maintain some level of rhythmicity. This is supported by the fact that rhythmicity and sleep phenotypes were correlated in the mutant flies (Fig. S5D). Unfortunately, heat shock alone had a strong effect on the sleep structure and lowered p-wake significantly in controls. Therefore, no conclusions can be drawn about the adult-specific effect of PDF in maintaining p-wake (Fig. 4F). These data suggest that the heat-shock based methods are compatible with studying circadian behavior but are less suitable for studying sleep behavior.

We also combined CRISPR/Cas9 mutagenesis with a more general method of temporal regulation that affects the Gal4 and therefore controls all UAS-based strategies, the recently developed auxin-inducible gene expression system (AGES, (McClure et al., 2022)). It uses the traditional Gal4 repressor Gal80, which has been engineered to be regulated by auxin. Auxin is non-toxic and does not affect fly lifespan at the required concentrations (McClure et al., 2022). We combined the AGES system with the regular Cas9, *UAS-Cas9.P2*, along with *UAS-Pdf-g* and *UAS-mRFP* to label the LNvs with the *Pdf-Gal4* driver (Fig. S6A).

AGES sequesters GAL4 and thus inhibits expression from all UAS-transgenes without auxin feeding (Fig. S6A, (McClure et al., 2022)). Indeed, there is no to very low mRFP expression in cell bodies or processes without auxin feeding (Fig. 5A, S6B). However, expression must be non-zero, as some PDF mutagenesis is observed without auxin feeding (~2-fold reduction in PDF levels, Fig. 5A, B). Not surprisingly, auxin feeding leads to a much bigger effect - near loss of all PDF from cell bodies (>10-fold reduction) as well as processes (Fig. 5A, B, S6B).

The small-scale leaky mutagenesis without auxin feeding had only a minor effect on rhythmicity and sleep (Fig. 5C, D, E). However, auxin feeding caused a very strong effect on both rhythmicity and sleep just like the effect on PDF staining (Fig. 5D, E, S6C), and adult specific loss of PDF lowered p-wake (Fig. 5F). Auxin feeding alone had a very minor effect on PDF staining (20% reduction in cell bodies) and no effect on circadian behavior and sleep duration (Fig. 5A-E, S6B, C). There was a significant interaction between auxin feeding and expression of CRISPR reagents against PDF on p-wake ($p<0.001$, Two-way ANOVA; Fig 5F). We therefore conclude from the combination of AGES with the CRISPR system that most if not all aspects of PDF function on circadian behavior and sleep are adult specific.

Discussion

In this study we generated new UAS-3X-gRNA lines for cell-specific perturbation of three key circadian genes and combined them with defined Gal4 drivers to assay their function in defined subsets of clock neurons. We could reproduce the mutant phenotypes of *vri*, *cry* and *Pdf* in known neurons and identified previously unknown cell-type specific functions of these genes. The approach worked very well with specific and weak Gal4 drivers, which allowed the discovery of two subsets of circadian neurons within which CRY acts independently to regulate rhythmicity under constant light conditions. Finally, these new reagents were compatible with existing tools and shown to be highly effective with two independent methods for temporal regulation. The results and lines described here will be of use to the circadian community, but we hope that the detailed validation of the method will appeal to a much wider population of fly neuroscientists and encourage them to switch from the standard but less dependable RNAi methodology to this more effective and consistent method for the spatial and temporal knockout of genes in adult fly neurons.

Our data show that this cell-type specific CRISPR method works well with highly expressed genes like *Pdf* and even with weak split Gal4 drivers. It is also ideal for addressing the adult function of essential genes such as *vri*, by perturbing their expression levels and function in inessential cells as we show here for circadian neurons. In this context, the functions of many *Drosophila* genes are defined only in developmental contexts, even though these same genes are expressed again in adults. For example, we recently found that genes encoding GPCRs, transcription factors and cell surface molecules are broadly yet specifically expressed in clock and dopaminergic neurons. Studying their function in these specific adult neurons is beginning to help define the molecular underpinnings of neural circuits and behavior (Ma et al., 2021, 2023). Towards these goals, we have generated and begun to use a library of guideRNA lines against all

GPCRs expressed in *Drosophila* (Schlichting et al., 2022). Moreover, several lines with 2X-gRNA generated by Port and Boutros (Port et al., 2020) are now publicly available. Such resources should also make this method a first choice for tissue and cell-type specific forward genetic screens.

Another novel application of this method should be cell-specific gene-interaction studies. Combining multiple RNAi lines is not common, perhaps because of the suspected dilution effects of multiple UAS lines. In contrast, this CRISPR/Cas9 method does not require high expression levels, so combining gRNAs against multiple genes, for example to study enhancer and suppressor phenotypes, should be possible and would extend the approach in an interesting direction.

VRI operates as a part of the molecular transcription translation feedback loop that operates in clock neurons (Cyran et al., 2003). Hemizygous mutants of *vri* are rhythmic with a short circadian period (Blau and Young, 1999). Concurrently, a recent study generated a new homozygous mutant that has normal rhythms with a short circadian period despite dramatically reduced VRI levels in the clock neurons (Gunawardhana et al., 2021). These results are in complete agreement with ours (Fig. 1C-E). An earlier study from the same laboratory used cell-specific flip outs to suggest a *vri* requirement for rhythmic behavior, but this result could have been influenced by the mutant background (Gunawardhana and Hardin, 2017). Although over-expression of VRI also results in considerable loss of rhythms (Blau and Young, 1999), simple loss of function via these CRISPR/Cas9-based method is less prone to misinterpretation than gain-of-function experiments. In the future, guides can be targeted to specific subsets of circadian and non-circadian cells to further define the function of VRI in the regulation of development and behavior.

The CRY photoreceptor along with the compound eyes and H-B eyelets are the three pathways through which flies entrain to environmental light cues (Helfrich-Förster et al., 2001). It is therefore not surprising that *cry* mutants are still able to light entrain normally. However, these

mutants are rhythmic under constant bright light conditions, indicating a special role for CRY under prolonged light exposure conditions (Patrick Emery et al., 2000). CRY is expressed in several different clock neurons; they include the PDF neurons, a subset of evening cells (5th sLNv+3 LNds) and a subset of the DN1ps (Benito et al., 2008). Interestingly, we find that CRY functions in only specific subsets of these cells to regulate the response to constant light. CRY in the PDF positive LNvs has no more than a minor role in responding to constant light, like previous results with *per* overexpression (Murad et al., 2007). Because the sLNvs are directly downstream of the light responsive H-B eyelets (Schlichting et al., 2016), these neurons may be constantly electrically stimulated and their molecular clock therefore poisoned by constant light even without CRY. In contrast, loss of CRY in either of the two other major subsets of CRY-positive neurons, the two evening cells (5th sLNv, CRY^{+} and ITP^{+} LNd) as well as the DN1ps, is sufficient to maintain rhythmicity in constant light. These data indicate that CRY maybe the primary source of light information in these neurons; perhaps they are critical for adapting to altered photoperiods such as longer summer days. The different period phenotypes suggest that CRY function in these two sets of neurons may segregate the evening delay and morning advance of the phase shift response (Kistenpfennig et al., 2012). CRY is also reported to regulate neuronal firing (Fogle et al., 2011), so altered electrical properties of the CRY mutants might also contribute to the observed period phenotypes.

Expression of *UAS-Cas9* and *UAS-Pdf-g* with *Pdf-Gal4* resulted in complete loss of PDF from sLNvs and a significant but partial loss from the lLNvs (Fig. 3A, B). The higher levels of PDF in the lLNvs is one possible explanation, but persistent PDF expression in lLNvs might also reflect the duration of expression of the CRISPR tools in the different cells. The sLNvs have an early larval origin, well before the lLNvs appear in the mid-late pupal stage (Helfrich-Förster,

1997). This temporal pattern is recapitulated by *Pdf-Gal4* (Renn et al., 1999), allowing sLNvs a much longer time for mutagenesis and protein turnover.

PDF is a key circadian neuropeptide in *Drosophila*. As small PDF neurons or the sLNvs are critical for circadian behavior (Grima et al., 2004; Stoleru et al., 2004), it is not surprising that PDF from the sLNvs is the key regulator of rhythmicity in constant darkness. The results here also show that loss of PDF from the lLNvs leads to a small effect on sleep structure as loss of PDF from the sLNvs, namely, a decrease in p-wake (Fig. 3H, K). This indicates that PDF from both sources is wake-promoting, consistent with the activation of lLNvs mediating arousal (Shang et al., 2008; Sheeba et al., 2008). Another possibility is that PDF from the large cells interacts with the PDF receptor present on the small cells, i.e., that the cells function in series rather than in parallel to promote wake.

Two independent methods indicate that PDF functions adult-specifically to regulate rhythmicity and sleep. Although both work effectively, the two strategies had distinguishing features. The inducible Cas9 system was very robust i.e., there was no leaky expression, which provides high confidence in the adult-specific conclusion. However, the induction was incomplete, leading to some mosaicism and high variance in the resulting phenotypes (Fig. S5A). Perhaps this could be solved by further altering the heat shock regimen, especially for rhythmicity as this assay is insensitive to the brief heat shock. Effects on sleep in contrast are more problematic, as this behavior is impacted by heat shock (Fig. 4F).

In contrast to heat shock, the auxin-inducible AGES system was highly efficient but exhibited some background mutagenesis in the absence of auxin. As the AGES system was highly effective at inhibiting the expression of a fluorescent protein marker (Fig. 5A, S6B), the background mutagenesis likely reflects the ability of even very low levels of Cas9 and gRNA

expression to induce mutagenesis. While the sensitivity of mutagenesis is a potential liability in this specific context, it is a generally positive feature of the CRISPR-based system, since it does not require that drivers be highly expressed to mediate efficient mutagenesis. In the context of AGES, the use of lower expression Cas9 variants (Port et al., 2020) might help circumvent this limitation. Importantly, auxin exposure alone had no detectable effect on circadian or sleep behavior. Thus, we find auxin exposure to be a less disruptive perturbation than heat shock and hence a mode of CRISPR induction more compatible for behavior analyses. Moreover, temporal regulation via AGES allows combining with other UAS transgenes for experiments like complementation analysis. However, the current version of AGES is incompatible with the many Gal80-insensitive split-Gal4 lines, which are so useful for restricted brain expression (Luan et al., 2006). In summary, both methods are effective with some differences, and we hope this analysis will help researchers choose the method best suited to their needs.

Materials and Methods

Fly Stocks and Rearing

All flies were raised on a standard cornmeal media supplemented with yeast in a temperature controlled incubator at 25°C in 12:12 Light:Dark cycles. The genotypes of all fly strains used in this study are listed in supplementary Table S1.

Generation of Fly Lines

To generate lines expressing 3X-guides under UAS-control, we used previously described protocols (Port and Bullock, 2016; Schlichting et al., 2019). Briefly, gRNAs specific to the target genes were identified using the CRISPR Optimal Target Finder tool (Gratz et al., 2014). These gRNA sequences were incorporated into the tRNA backbone using 2 PCR reactions, primers for which are listed in supplementary Table S2. The PCR products were assembled into the UASpCFD6 vector (Addgene #73915) digested with BbsI-HF enzyme (NEB) using Gibson assembly. Sequence verified plasmids were injected into the attP2 site on the third chromosome by Rainbow Transgenic Flies Inc (Camarillo, CA, USA). Positive transformants were screened for by red eye color based on the miniwhite marker.

Locomotor Activity and Sleep Behavior

For behavior analysis of flies with non-adult specific perturbations, 0-3 days old male flies of the appropriate genotype were collected and aged till they were about 2 weeks old at 25°C in 12:12 LD, with food changes every 3-4 days. The flies were then loaded into behavior tubes containing food (4% sucrose and 2% agar) and loaded onto *Drosophila* Activity Monitors (DAM; TriKinetics Inc., Waltham, MA). These DAMs were placed in light boxes with programmable LED light

intensities inside a temperature-controlled incubator set to 25°C. Flies were entrained for 2-3 days with 12h:12h lights ON (500 lux): lights OFF before being switched to either constant darkness or constant light (500 lux). Circadian rhythmicity and sleep analysis was performed using the 2020 version of Sleep and Circadian Analysis MATLAB Program (SCAMP) developed by Christopher G. Vecsey (Donelson et al., 2012). For period analysis, only rhythmic flies (Rhythmicity Index > 0.25) were used. E-peak timing was calculated as the highest point in bins from ZT6.5-ZT10.5 of average activity in 30 min bins exported from SCAMP. Sleep structure analysis for p-wake and p-doze (Wiggin et al., 2020) was also performed using this new version of SCAMP.

For experiments with the inducible Cas9 system, 2-5 days old male flies of the appropriate genotype were heat shocked on 3 consecutive days. The first heat shock was 25 mins, and the two subsequent ones were 40 mins each. Heat shock was delivered by placing flies in an empty food vial and submerging the vial in a water bath set at 37°C. Flies were removed promptly and allowed to recover briefly at room temperature before being transferred to a fresh vial with standard cornmeal food. Once the flies recovered completely, the flies were placed in an incubator set to 25°C. Flies were aged for 2 weeks from the day of the first heat shock before loading them in behavior experiments. Control flies were collected at the same time and aged simultaneously but without the heat shock.

For AGES experiments, 2-5 days old male flies were fed Instant *Drosophila* Medium (Formula 424®, Carolina) reconstituted either in 10mM Auxin (GK2088, Glentham Life Sciences) or distilled water (for controls). Flies were fed this food for about 2 weeks before loading them in behavior tubes with standard behavior food (4% sucrose and 2% agar). Since CRISPR based mutagenesis irreversibly alters the DNA in the cells of interest, we used standard behavior food for behavior analysis post auxin feeding to make experiments simpler.

Immunohistochemistry and Image Analysis

Whole flies of the same genotype and age as the behavior experiment cohort were fixed at ZT18-19 in 4% paraformaldehyde in PBS with 0.4% Triton X-100 for 2 hours and 30 minutes at room temperature. Tubes were wrapped in tin foil to protect them from light while rotating on a shaker. Flies were then washed three times (10 minutes each) with 0.4% PBST before dissecting the brain. Dissected brains were washed and blocked with 10% Normal Goat Serum (NGS; Jackson labs) in 0.4% PBST (blocking buffer) for 2 hours at room temperature or at 4°C overnight. The following primary antibodies were used diluted in blocking buffer– chicken anti-GFP (Abcam ab13970; 1:1000), mouse anti-PDF (DSHB-PDF C7; 1:1000), guinea pig anti-VRI (gift of Paul Hardin; 1:3000 (Glossop et al., 2003)), rat anti-TIM (Rosbash lab; 1:250), rabbit anti-dsRed (Takara Bio-632393; 1:300) and rat anti-RFP (Proteintech-5f8; 1:1000). Primary antibody was incubated for 24-36 hours at 4°C. The brains were then washed three times (30 minutes each) in 0.4% PBST, corresponding secondary antibodies were used at a 1:500 dilution in blocking buffer and incubated at 4°C overnight. Brains were again washed three times (30 minutes each) in 0.4% PBS, mounted in VectaShield mounting medium (Vector Laboratories).

Images were acquired using Leica Stellaris 8 confocal microscope equipped with a white light laser. Images for one set of experiments were acquired using the Leica SP5 confocal microscope. For each experiment, the laser settings were kept constant across genotypes. Either 20X air objective or a 40X oil objective (for image quantification) with NA of 1.43 was used.

Image analysis was performed with Fiji (Schindelin et al., 2012) using the Time Analyzer V3 plugin to mark ROIs across channels and measure intensity of the PDF channel. Background intensity for a z-stack was measured from three random background regions, averaged, and subtracted from each ROI.

Data representation and Statistical Analysis

Some of the figure panels (Fig. S3A, S5A and S6A) were created using BioRender.com. Boxplots were generated using BoxPlotR (Spitzer et al., 2014). For all boxplots, center lines show the medians; box limits indicate the 25th and 75th percentiles as determined by R software; whiskers extend 1.5 times the interquartile range from the 25th and 75th percentiles, outliers are represented by dots. All statistical tests were performed using the free online tool Statistics Kingdom https://www.statskingdom.com/index.html

Acknowledgements

We thank Michelle Lin for assistance with maintaining fly stocks. We thank Matthias Schlichting and all members of the Rosbash lab for useful discussions. We thank Paul Garrity, Justin Blau and Katharine Abruzzi for helpful comments on the manuscript. We thank Paul Hardin for the VRI antibody. We thank Heather Dionne, Aljoscha Nern and Gerry Rubin (Janelia Research campus) for the split-Gal4 lines, and Filip Port and Michael Boutros for the STOP-Cas9 flies. Flies from *Drosophila* Genomics Research Center (DGRC- NIH P40OD018537) and Vienna Drosophila Resource Center (VDRC) were used in this study. This work was supported by the Howard Hughes Medical Institute (HHMI).

References

Allada R, Chung BY. 2010. Circadian Organization of Behavior and Physiology in Drosophila. *Annu Rev Physiol* **72**:605–624. doi:10.1146/annurev-physiol-021909-135815

Bahn JH, Lee G, Park JH. 2009. Comparative Analysis of Pdf-Mediated Circadian Behaviors Between Drosophila melanogaster and D. virilis. *Genetics* **181**:965–975. doi:10.1534/genetics.108.099069

Benito J, Houl JH, Roman GW, Hardin PE. 2008. The blue light photoreceptor CRYPTOCHROME is expressed in a subset of circadian oscillator neurons in the Drosophila CNS. *J Biol Rhythms* **23**:296–307. doi:10.1177/0748730408318588

Blau J, Young MW. 1999. Cycling vrille expression is required for a functional Drosophila clock. *Cell* **99**:661–671. doi:10.1016/s0092-8674(00)81554-8

Brand AH, Perrimon N. 1993. Targeted gene expression as a means of altering cell fates and generating dominant phenotypes. *Dev Camb Engl* **118**:401–415. doi:10.1242/dev.118.2.401

Bulthuis N, Spontak KR, Kleeman B, Cavanaugh DJ. 2019. Neuronal Activity in Non-LNv Clock Cells is Required to Produce Free-Running Rest:Activity Rhythms in Drosophila. *J Biol Rhythms* **34**:249–271. doi:10.1177/0748730419841468

Cyran SA, Buchsbaum AM, Reddy KL, Lin M-C, Glossop NRJ, Hardin PE, Young MW, Storti RV, Blau J. 2003. vrille, Pdp1, and dClock Form a Second Feedback Loop in the Drosophila Circadian Clock. *Cell* **112**:329–341. doi:10.1016/S0092-8674(03)00074-6

Delventhal R, O'Connor RM, Pantalia MM, Ulgherait M, Kim HX, Basturk MK, Canman JC, Shirasu-Hiza M. 2019. Dissection of central clock function in Drosophila through cell-specific CRISPR-mediated clock gene disruption. *eLife* **8**:e48308. doi:10.7554/eLife.48308

Dietzl G, Chen D, Schnorrer F, Su K-C, Barinova Y, Fellner M, Gasser B, Kinsey K, Oppel S, Scheiblauer S, Couto A, Marra V, Keleman K, Dickson BJ. 2007. A genome-wide transgenic RNAi library for conditional gene inactivation in Drosophila. *Nature* **448**:151–156. doi:10.1038/nature05954

Donelson N, Kim EZ, Slawson JB, Vecsey CG, Huber R, Griffith LC. 2012. High-Resolution Positional Tracking for Long-Term Analysis of Drosophila Sleep and Locomotion Using the "Tracker" Program. *PLOS ONE* **7**:e37250. doi:10.1371/journal.pone.0037250

Dubowy C, Sehgal A. 2017. Circadian Rhythms and Sleep in Drosophila melanogaster. *Genetics* **205**:1373–1397. doi:10.1534/genetics.115.185157

Emery P, So WV, Kaneko M, Hall JC, Rosbash M. 1998. CRY, a Drosophila Clock and Light-Regulated Cryptochrome, Is a Major Contributor to Circadian Rhythm Resetting and Photosensitivity. *Cell* **95**:669–679. doi:10.1016/S0092-8674(00)81637-2

Emery Patrick, Stanewsky R, Hall JC, Rosbash M. 2000. A unique circadian-rhythm photoreceptor. *Nature* **404**:456–457. doi:10.1038/35006558

Emery P., Stanewsky R, Helfrich-Förster C, Emery-Le M, Hall JC, Rosbash M. 2000. Drosophila CRY is a deep brain circadian photoreceptor. *Neuron* **26**:493–504. doi:10.1016/s0896-6273(00)81181-2

Fogle KJ, Parson KG, Dahm NA, Holmes TC. 2011. CRYPTOCHROME Is a Blue-Light Sensor That Regulates Neuronal Firing Rate. *Science* **331**:1409–1413. doi:10.1126/science.1199702

George H, Terracol R. 1997. The vrille Gene of Drosophila Is a Maternal Enhancer of decapentaplegic and Encodes a New Member of the bZIP Family of Transcription Factors. *Genetics* **146**:1345–1363. doi:10.1093/genetics/146.4.1345

Glossop NRJ, Houl JH, Zheng H, Ng FS, Dudek SM, Hardin PE. 2003. VRILLE feeds back to control circadian transcription of Clock in the Drosophila circadian oscillator. *Neuron* **37**:249–261. doi:10.1016/s0896-6273(03)00002-3

Gratz SJ, Ukken FP, Rubinstein CD, Thiede G, Donohue LK, Cummings AM, O'Connor-Giles KM. 2014. Highly specific and efficient CRISPR/Cas9-catalyzed homology-directed repair in Drosophila. *Genetics* **196**:961–971. doi:10.1534/genetics.113.160713

Grima B, Chélot E, Xia R, Rouyer F. 2004. Morning and evening peaks of activity rely on different clock neurons of the Drosophila brain. *Nature* **431**:869–873. doi:10.1038/nature02935

Gunawardhana KL, Hardin PE. 2017. VRILLE Controls PDF Neuropeptide Accumulation and Arborization Rhythms in Small Ventrolateral Neurons to Drive Rhythmic Behavior in Drosophila. *Curr Biol* **27**:3442-3453.e4. doi:10.1016/j.cub.2017.10.010

Gunawardhana KL, Rivas GBS, Caster C, Hardin PE. 2021. Crosstalk between vrille transcripts, proteins, and regulatory elements controlling circadian rhythms and development in Drosophila. *iScience* **24**. doi:10.1016/j.isci.2020.101893

Guo F, Chen X, Rosbash M. 2017. Temporal calcium profiling of specific circadian neurons in freely moving flies. *Proc Natl Acad Sci U S A* **114**:E8780–E8787. doi:10.1073/pnas.1706608114

Guo F, Holla M, Díaz MM, Rosbash M. 2018. A Circadian Output Circuit Controls Sleep-Wake Arousal in Drosophila. *Neuron* **100**:624-635.e4. doi:10.1016/j.neuron.2018.09.002

Guo F, Yu J, Jung HJ, Abruzzi KC, Luo W, Griffith LC, Rosbash M. 2016. Circadian neuron feedback controls the Drosophila sleep–activity profile. *Nature* **536**:292–297. doi:10.1038/nature19097

Hardin PE. 2011. Molecular genetic analysis of circadian timekeeping in Drosophila. *Adv Genet* **74**:141–173. doi:10.1016/B978-0-12-387690-4.00005-2

Helfrich-Förster C. 2003. The neuroarchitecture of the circadian clock in the brain of Drosophila melanogaster. *Microsc Res Tech* **62**:94–102. doi:10.1002/jemt.10357

Helfrich-Förster C. 1997. Development of pigment-dispersing hormone-immunoreactive neurons in the nervous system of Drosophila melanogaster. *J Comp Neurol* **380**:335–354. doi:10.1002/(SICI)1096-9861(19970414)380:3<335::AID-CNE4>3.0.CO;2-3

Helfrich-Förster C, Winter C, Hofbauer A, Hall JC, Stanewsky R. 2001. The Circadian Clock of Fruit Flies Is Blind after Elimination of All Known Photoreceptors. *Neuron* **30**:249–261. doi:10.1016/S0896-6273(01)00277-X

Jinek M, Chylinski K, Fonfara I, Hauer M, Doudna JA, Charpentier E. 2012. A Programmable Dual-RNA–Guided DNA Endonuclease in Adaptive Bacterial Immunity. *Science* **337**:816–821. doi:10.1126/science.1225829

King AN, Sehgal A. 2020. Molecular and circuit mechanisms mediating circadian clock output in the Drosophila brain. *Eur J Neurosci* **51**:268–281. doi:10.1111/ejn.14092

Kistenpfennig C, Hirsh J, Yoshii T, Helfrich-Förster C. 2012. Phase-shifting the fruit fly clock without cryptochrome. *J Biol Rhythms* **27**:117–125. doi:10.1177/0748730411434390

Li Q, Stavropoulos N. 2016. Evaluation of Ligand-Inducible Expression Systems for Conditional Neuronal Manipulations of Sleep in Drosophila. *G3 GenesGenomesGenetics* **6**:3351–3359. doi:10.1534/g3.116.034132

Luan H, Peabody NC, Vinson CR, White BH. 2006. Refined Spatial Manipulation of Neuronal Function by Combinatorial Restriction of Transgene Expression. *Neuron* **52**:425–436. doi:10.1016/j.neuron.2006.08.028

Ma D, Herndon N, Le JQ, Abruzzi KC, Zinn K, Rosbash M. 2023. Neural connectivity molecules best identify the heterogeneous clock and dopaminergic cell types in the Drosophila adult brain. *Sci Adv* **9**:eade8500. doi:10.1126/sciadv.ade8500

Ma D, Przybylski D, Abruzzi KC, Schlichting M, Li Q, Long X, Rosbash M. 2021. A transcriptomic taxonomy of Drosophila circadian neurons around the clock. *eLife* **10**:e63056. doi:10.7554/eLife.63056

Matsumoto A, Ukai-Tadenuma M, Yamada RG, Houl J, Uno KD, Kasukawa T, Dauwalder B, Itoh TQ, Takahashi K, Ueda R, Hardin PE, Tanimura T, Ueda HR. 2007. A functional genomics strategy reveals *clockwork orange* as a transcriptional regulator in the *Drosophila* circadian clock. *Genes Dev* **21**:1687–1700. doi:10.1101/gad.1552207

McClure CD, Hassan A, Aughey GN, Butt K, Estacio-Gómez A, Duggal A, Ying Sia C, Barber AF, Southall TD. 2022. An auxin-inducible, GAL4-compatible, gene expression system for Drosophila. *eLife* **11**:e67598. doi:10.7554/eLife.67598

Meissner GW, Nern A, Dorman Z, DePasquale GM, Forster K, Gibney T, Hausenfluck JH, He Y, Iyer N, Jeter J, Johnson L, Johnston RM, Lee K, Melton B, Yarbrough B, Zugates CT, Clements J, Goina C, Otsuna H, Rokicki K, Svirskas RR, Aso Y, Card GM, Dickson BJ, Ehrhardt E, Goldammer J, Ito M, Kainmueller D, Korff W, Mais L, Minegishi R, Namiki S, Rubin GM, Sterne GR, Wolff T, Malkesman O, Team FP. 2022. A searchable image resource of Drosophila GAL4-driver expression patterns with single neuron resolution. doi:10.1101/2020.05.29.080473

Meltzer H, Marom E, Alyagor I, Mayseless O, Berkun V, Segal-Gilboa N, Unger T, Luginbuhl D, Schuldiner O. 2019. Tissue-specific (ts)CRISPR as an efficient strategy for in vivo screening in Drosophila. *Nat Commun* **10**:2113. doi:10.1038/s41467-019-10140-0

Murad A, Emery-Le M, Emery P. 2007. A Subset of Dorsal Neurons Modulates Circadian Behavior and Light Responses in Drosophila. *Neuron* **53**:689–701. doi:10.1016/j.neuron.2007.01.034

Osterwalder T, Yoon KS, White BH, Keshishian H. 2001. A conditional tissue-specific transgene expression system using inducible GAL4. *Proc Natl Acad Sci* **98**:12596–12601. doi:10.1073/pnas.221303298

Parisky KM, Agosto J, Pulver SR, Shang Y, Kuklin E, Hodge JJL, Kang K, Liu X, Garrity PA, Rosbash M, Griffith LC. 2008. PDF cells are a GABA-responsive wake-

promoting component of the Drosophila sleep circuit. *Neuron* **60**:672–682. doi:10.1016/j.neuron.2008.10.042

Parisky KM, Agosto Rivera JL, Donelson NC, Kotecha S, Griffith LC. 2016. Reorganization of Sleep by Temperature in Drosophila Requires Light, the Homeostat, and the Circadian Clock. *Curr Biol CB* **26**:882–892. doi:10.1016/j.cub.2016.02.011

Port F, Boutros M. 2022. Tissue-Specific CRISPR-Cas9 Screening in Drosophila. *Methods Mol Biol Clifton NJ* **2540**:157–176. doi:10.1007/978-1-0716-2541-5_7

Port F, Bullock SL. 2016. Augmenting CRISPR applications in Drosophila with tRNA-flanked sgRNAs. *Nat Methods* **13**:852–854. doi:10.1038/nmeth.3972

Port F, Chen H-M, Lee T, Bullock SL. 2014. Optimized CRISPR/Cas tools for efficient germline and somatic genome engineering in Drosophila. *Proc Natl Acad Sci U S A* **111**:E2967-2976. doi:10.1073/pnas.1405500111

Port F, Strein C, Stricker M, Rauscher B, Heigwer F, Zhou J, Beyersdörffer C, Frei J, Hess A, Kern K, Lange L, Langner N, Malamud R, Pavlović B, Rädecke K, Schmitt L, Voos L, Valentini E, Boutros M. 2020. A large-scale resource for tissue-specific CRISPR mutagenesis in Drosophila. *eLife* **9**:e53865. doi:10.7554/eLife.53865

Renn SC, Park JH, Rosbash M, Hall JC, Taghert PH. 1999. A pdf neuropeptide gene mutation and ablation of PDF neurons each cause severe abnormalities of behavioral circadian rhythms in Drosophila. *Cell* **99**:791–802. doi:10.1016/s0092-8674(00)81676-1

Schindelin J, Arganda-Carreras I, Frise E, Kaynig V, Longair M, Pietzsch T, Preibisch S, Rueden C, Saalfeld S, Schmid B, Tinevez J-Y, White DJ, Hartenstein V, Eliceiri K, Tomancak P, Cardona A. 2012. Fiji: an open-source platform for biological-image analysis. *Nat Methods* **9**:676–682. doi:10.1038/nmeth.2019

Schlichting M, Díaz MM, Xin J, Rosbash M. 2019. Neuron-specific knockouts indicate the importance of network communication to Drosophila rhythmicity. *eLife* **8**:e48301. doi:10.7554/eLife.48301

Schlichting M, Menegazzi P, Lelito KR, Yao Z, Buhl E, Benetta ED, Bahle A, Denike J, Hodge JJ, Helfrich-Förster C, Shafer OT. 2016. A Neural Network Underlying Circadian Entrainment and Photoperiodic Adjustment of Sleep and Activity in Drosophila. *J Neurosci* **36**:9084–9096. doi:10.1523/JNEUROSCI.0992-16.2016

Schlichting M, Richhariya S, Herndon N, Ma D, Xin J, Lenh W, Abruzzi K, Rosbash M. 2022. Dopamine and GPCR-mediated modulation of DN1 clock neurons gates the circadian timing of sleep. *Proc Natl Acad Sci* **119**:e2206066119. doi:10.1073/pnas.2206066119

Schubert FK, Hagedorn N, Yoshii T, Helfrich-Förster C, Rieger D. 2018. Neuroanatomical details of the lateral neurons of Drosophila melanogaster support their functional role in the circadian system. *J Comp Neurol* **526**:1209–1231. doi:10.1002/cne.24406

Sekiguchi M, Inoue K, Yang T, Luo D-G, Yoshii T. 2020. A Catalog of GAL4 Drivers for Labeling and Manipulating Circadian Clock Neurons in Drosophila melanogaster. *J Biol Rhythms* **35**:207–213. doi:10.1177/0748730419895154

Shafer OT, Taghert PH. 2009. RNA-Interference Knockdown of Drosophila Pigment Dispersing Factor in Neuronal Subsets: The Anatomical Basis of a

Neuropeptide's Circadian Functions. *PLOS ONE* **4**:e8298. doi:10.1371/journal.pone.0008298

Shang Y, Griffith LC, Rosbash M. 2008. Light-arousal and circadian photoreception circuits intersect at the large PDF cells of the Drosophila brain. *Proc Natl Acad Sci* **105**:19587–19594. doi:10.1073/pnas.0809577105

Sheeba V, Fogle KJ, Kaneko M, Rashid S, Chou Y-T, Sharma VK, Holmes TC. 2008. Large Ventral Lateral Neurons Modulate Arousal and Sleep in Drosophila. *Curr Biol CB* **18**:1537–1545. doi:10.1016/j.cub.2008.08.033

Stanewsky R, Kaneko M, Emery P, Beretta B, Wager-Smith K, Kay SA, Rosbash M, Hall JC. 1998. The cryb mutation identifies cryptochrome as a circadian photoreceptor in Drosophila. *Cell* **95**:681–692. doi:10.1016/s0092-8674(00)81638-4

Stoleru D, Peng Y, Agosto J, Rosbash M. 2004. Coupled oscillators control morning and evening locomotor behaviour of Drosophila. *Nature* **431**:862–868. doi:10.1038/nature02926

Wiggin TD, Goodwin PR, Donelson NC, Liu C, Trinh K, Sanyal S, Griffith LC. 2020. Covert sleep-related biological processes are revealed by probabilistic analysis in Drosophila. *Proc Natl Acad Sci U S A* **117**:10024–10034. doi:10.1073/pnas.1917573117

Yao Z, Shafer OT. 2014. The Drosophila circadian clock is a variably coupled network of multiple peptidergic units. *Science* **343**:1516–1520. doi:10.1126/science.1251285

Zhang L, Chung BY, Lear BC, Kilman VL, Liu Y, Mahesh G, Meissner R-A, Hardin PE, Allada R. 2010. DN1p Circadian Neurons Coordinate Acute Light and PDF Inputs to Produce Robust Daily Behavior in Drosophila. *Curr Biol* **20**:591–599. doi:10.1016/j.cub.2010.02.056

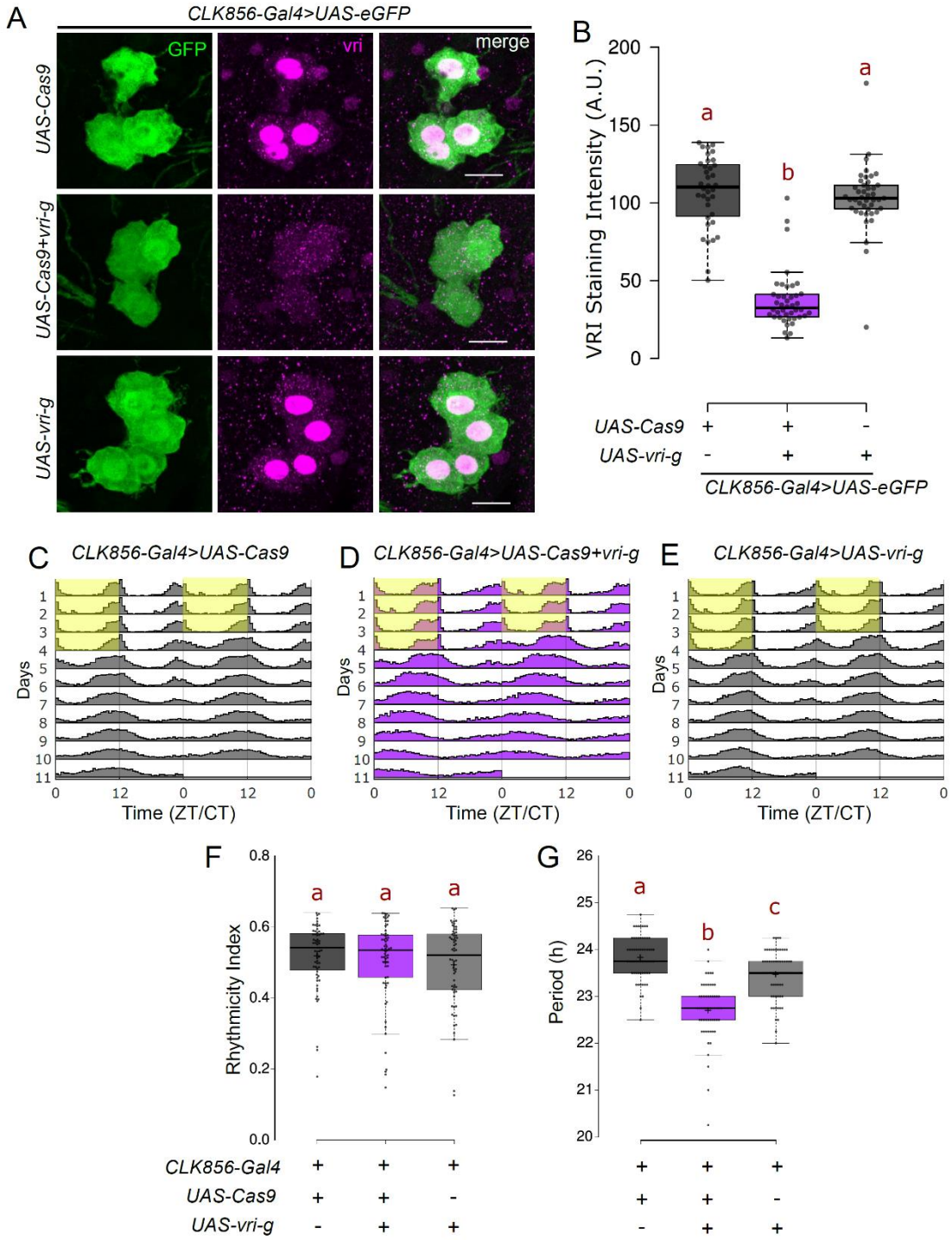

Fig. 1: Loss of VRI from clock neurons leads to a shorter circadian period.

A. Representative images of large LNV neurons stained for GFP and VRI at ZT19. There is loss of (nuclear) VRI staining in cells expressing both *UAS-Cas9* and UAS-3X-guides against *vri*

(UAS-vri-g). Some non-nuclear staining is visible in both control and mutant cells which could be due to background reactivity of the antibody. Scale bar represents 10µm. **B.** Quantification of VRI staining intensity from large LNv neurons represented as a boxplot, $n \geq 36$ cells from at least 12 hemibrains per genotype, letters represent statistically distinct groups; $p<0.001$, Kruskal Wallis test followed by a post hoc Dunn's test**. C-E**. Actograms represent double-plotted average activity of flies from an experiment across multiple days. Yellow panel indicates lights ON. F. Rhythmicity Index for individual flies plotted as a boxplot, $n \geq 62$ per genotype from at least two independent experiments. No statistical difference was observed among the groups tested ($p=0.6$, Kruskal Wallis test). E. Free running period under constant darkness for individual rhythmic flies ($RI>0.25$) plotted as a boxplot, letters represent statistically distinct groups; $p<0.01$, Kruskal Wallis test followed by a post hoc Dunn's test.

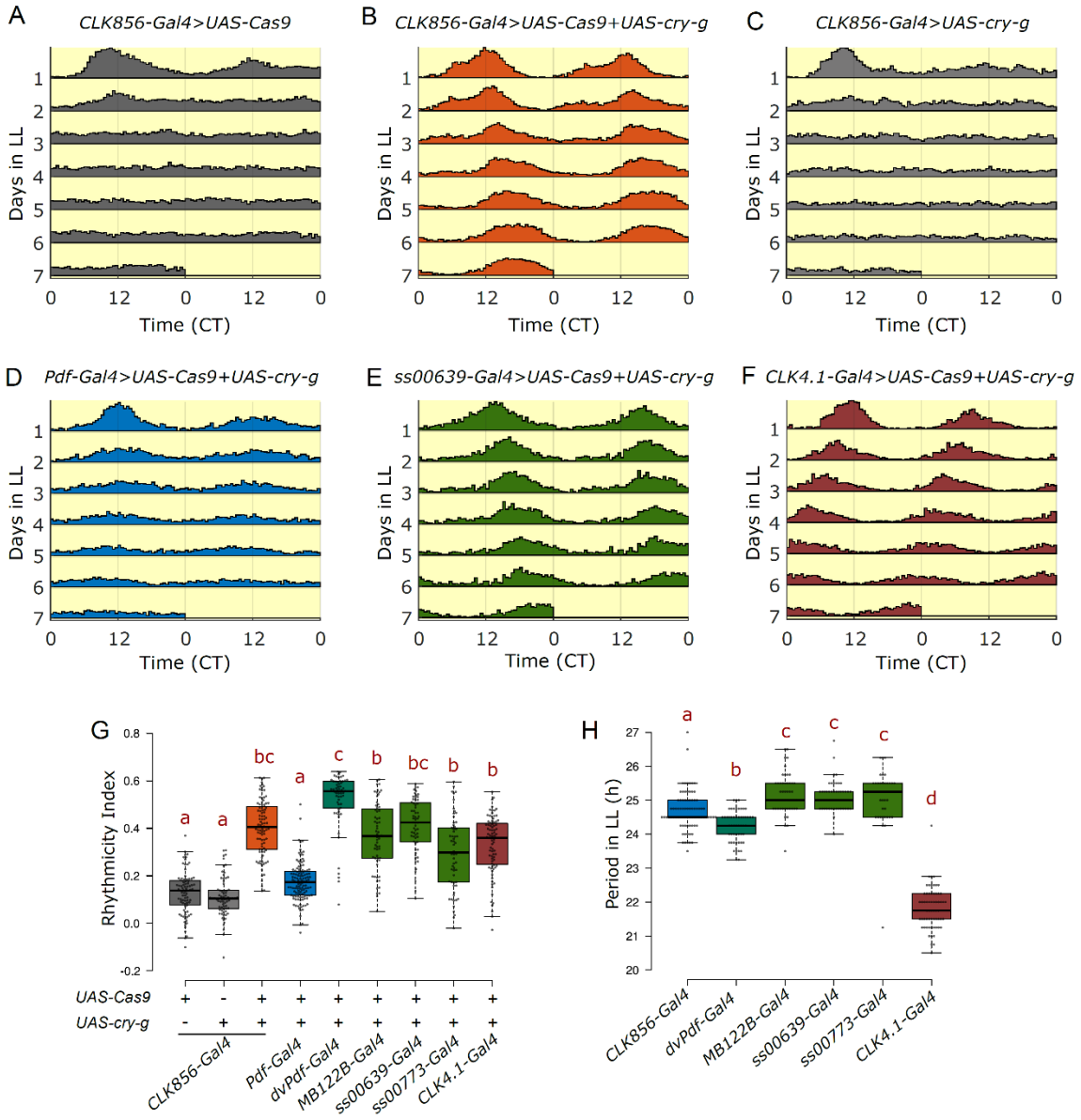

Fig. 2: CRY function in two discrete subsets of clock neurons can regulate rhythmicity under constant light conditions. A-F. Actograms represent double-plotted average activity of flies from an experiment across multiple days in constant light. Flies expressing both *UAS-Cas9* and UAS-3X-guides against *cry (UAS-cry-g)* in clock neurons are rhythmic in constant light conditions. **G**. Rhythmicity Index of individual flies quantified for LL2-7 represented by a boxplot, n ≥ 51 per genotype from at least two independent experiments. Letters represent statistically distinct groups; p<0.001, Kruskal Wallis test followed by a post hoc Dunn's test. **E**. Period under constant light

for individual rhythmic flies (Rhythmicity Index > 0.25) quantified for LL2-7 represented by a boxplot, letters represent statistically distinct groups; $p<0.01$, Kruskal Wallis test followed by a post hoc Dunn's test.

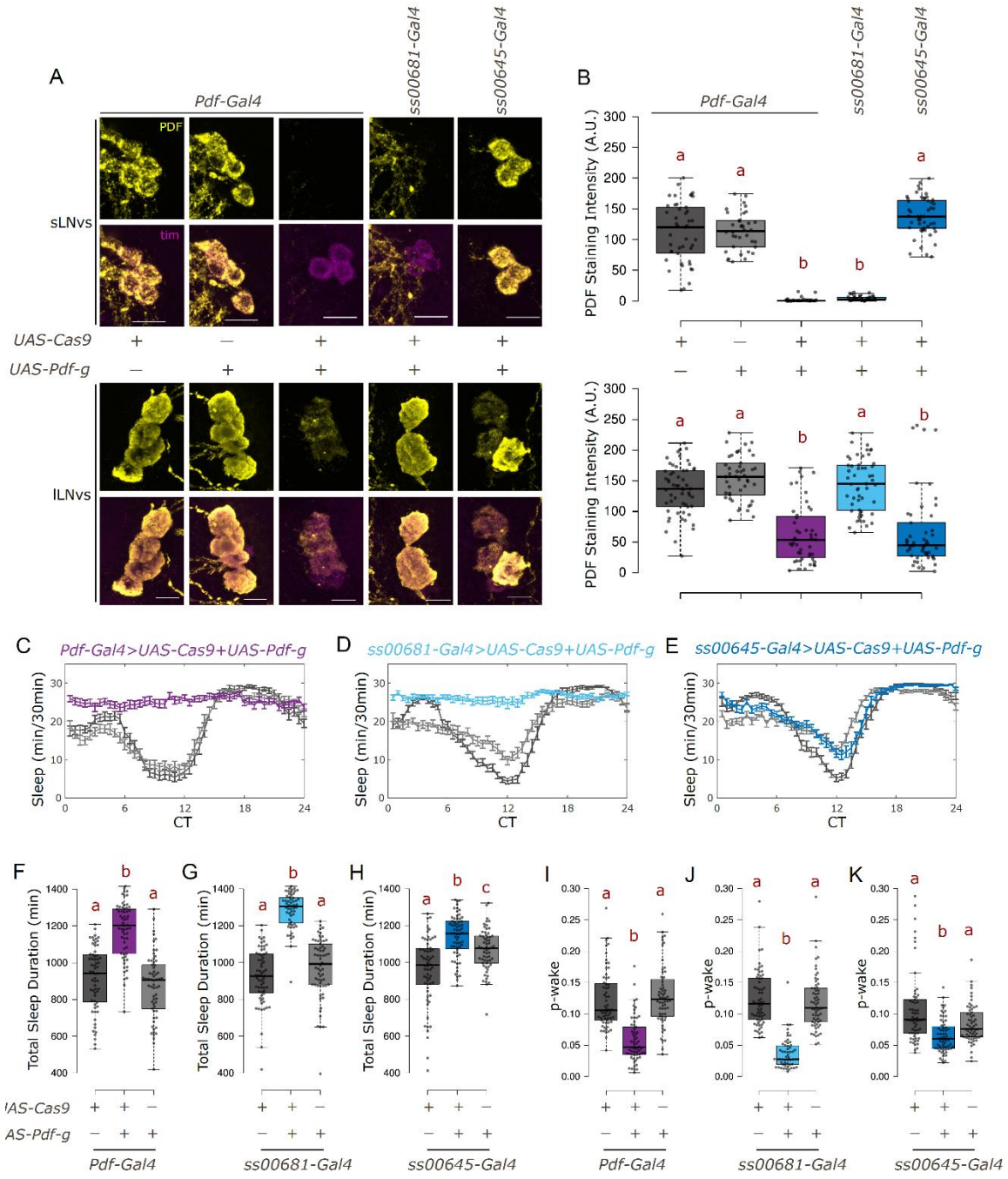

Fig. 3: PDF from sLNvs maintains wakefulness under constant darkness. A. Representative images of sLNvs (top) and lLNvs (bottom) stained for TIM and PDF at ZT18. There is loss of PDF staining in cells expressing both *UAS-Cas9* and UAS-3X-guides against *Pdf (UAS-Pdf-g)*. Scale bar represents 10µm. **B**. Quantification of PDF staining intensity from sLNv (top) and lLNv (bottom) neurons represented with boxplots, n ≥ 36 cells from at least 11 hemibrains per genotype.

Letters represent statistically distinct groups; $p<0.001$, Kruskal Wallis test followed by a post hoc Dunn's test. **C-E**. Sleep plots representing average sleep of flies from DD1-4 in 30-minute bins. *UAS-Cas9* alone control is indicated in dark gray, *UAS-Pdf-g* alone control in light gray whereas the experimental genotype expressing both is represented by color indicated above the plots. **F-H**. Total sleep duration in a day for individual flies quantified (from DD1-4) represented by a boxplot, $n \geq 55$ per genotype from at least two independent experiments. Letters represent statistically distinct groups, $p<0.01$; Kruskal Wallis test followed by a post hoc Dunn's test. **I-K**. P-wake over a 24-hour period for individual flies quantified (from DD1-4) represented by a boxplot, letters represent statistically distinct groups; $p<0.001$, Kruskal Wallis test followed by a post hoc Dunn's test.

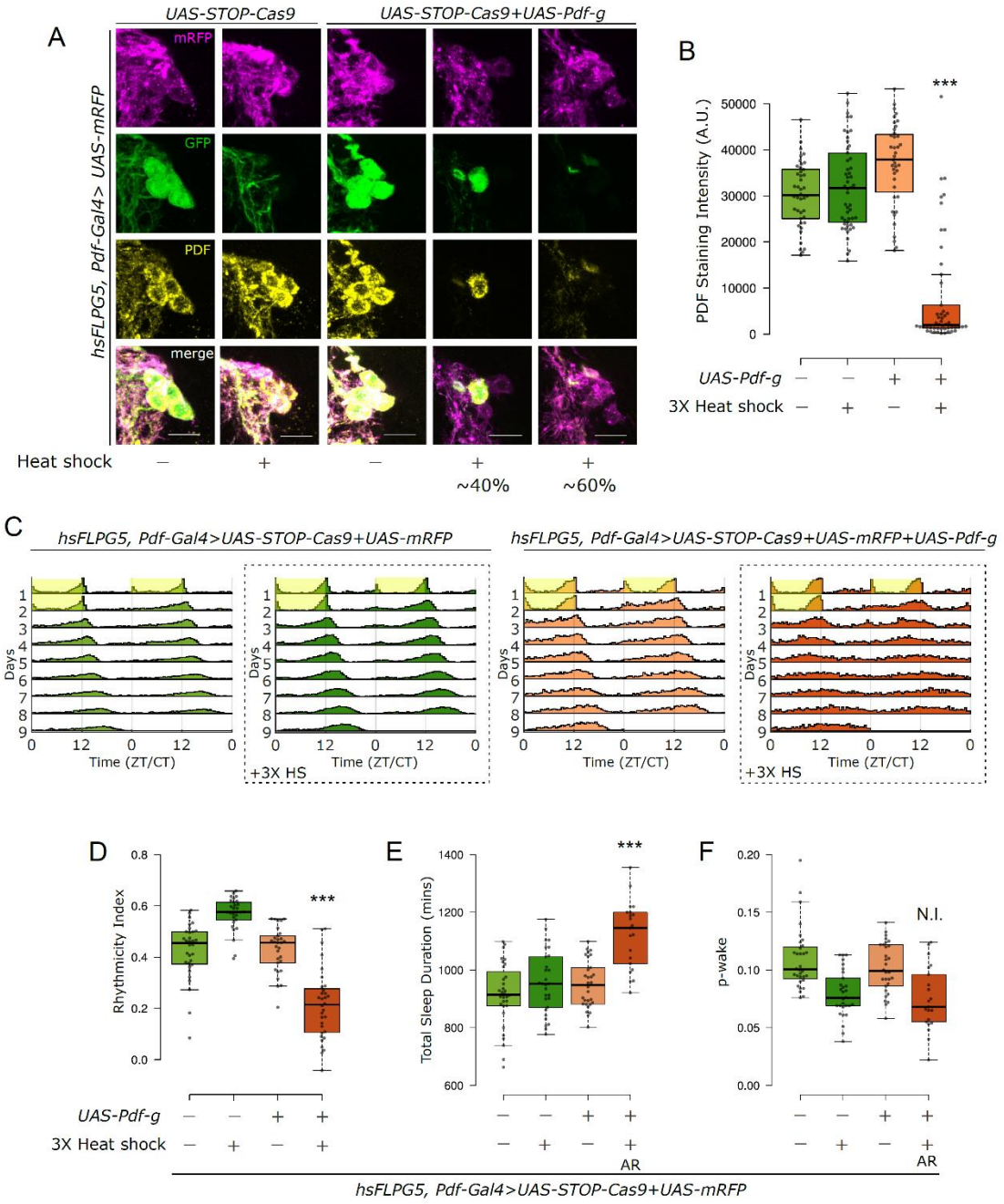

Fig. 4: Adult specific loss of PDF using an inducible Cas9 system results in loss of rhythmicity and increased sleep. A. Representative images of sLNvs stained for GFP, mRFP and PDF. 2 weeks post heat shock, there is loss of PDF staining in cells expressing both *UAS-Cas9* and *UAS-Pdf-g*. In about 60% of the hemibrains analyzed, PDF staining was lost from all sLNvs, whereas in the remaining 40% hemibrains, some mosaicism was observed as PDF staining was unchanged

in 1-2 sLNvs. Scale bar represents 10µm. **B**. Quantification of PDF staining intensity from sLNvs represented with boxplots, n ≥ 39 cells from at least 12 hemibrains per genotype/condition. There is a significant effect of both variables on the staining intensity and a significant interaction when CRISPR reagents for inducible CRISPR for *Pdf* were combined with 3X heat shock (Two-way ANOVA; *** Interaction p<0.001). **C**. Actograms represent double-plotted average activity of flies from an experiment across multiple days. Yellow panel indicates lights ON. Panels in dotted boxes indicate heat-shocked flies. **D**. Rhythmicity Index for individual flies quantified (from DD2-7) represented by a boxplot, n ≥ 29 per genotype. There is a significant effect of both variables on rhythmicity and a significant interaction when CRISPR reagents for inducible CRISPR for *Pdf* were combined with 3X heat shock (Two-way ANOVA; *** Interaction p<0.001). **E**. Total sleep duration in a day for individual flies quantified for DD1-4 represented by a boxplot. For the group expressing both *UAS-Cas9* and *UAS-Pdf-g* with heat-shock, only data from the arrhythmic flies are shown and used for statistics (indicated by AR). Also see Fig. S5D. There is a significant effect of both variables on sleep duration and a significant interaction when CRISPR reagents for inducible CRISPR for *Pdf* were combined with 3X heat shock (Two-way ANOVA; *** Interaction p<0.001). **F**. p-wake over a 24-hour period for individual flies quantified (from DD1-4) represented by a boxplot. For the group expressing both *UAS-Cas9* and *UAS-Pdf-g* with heat-shock, only data from the arrhythmic flies are shown and used for statistics (indicated by AR). Also see Fig. S5D. Only heat-shock had a significant effect on p-wake and there was no interaction between the variables (Two-way ANOVA; N.I. = No Interaction, p=0.31).

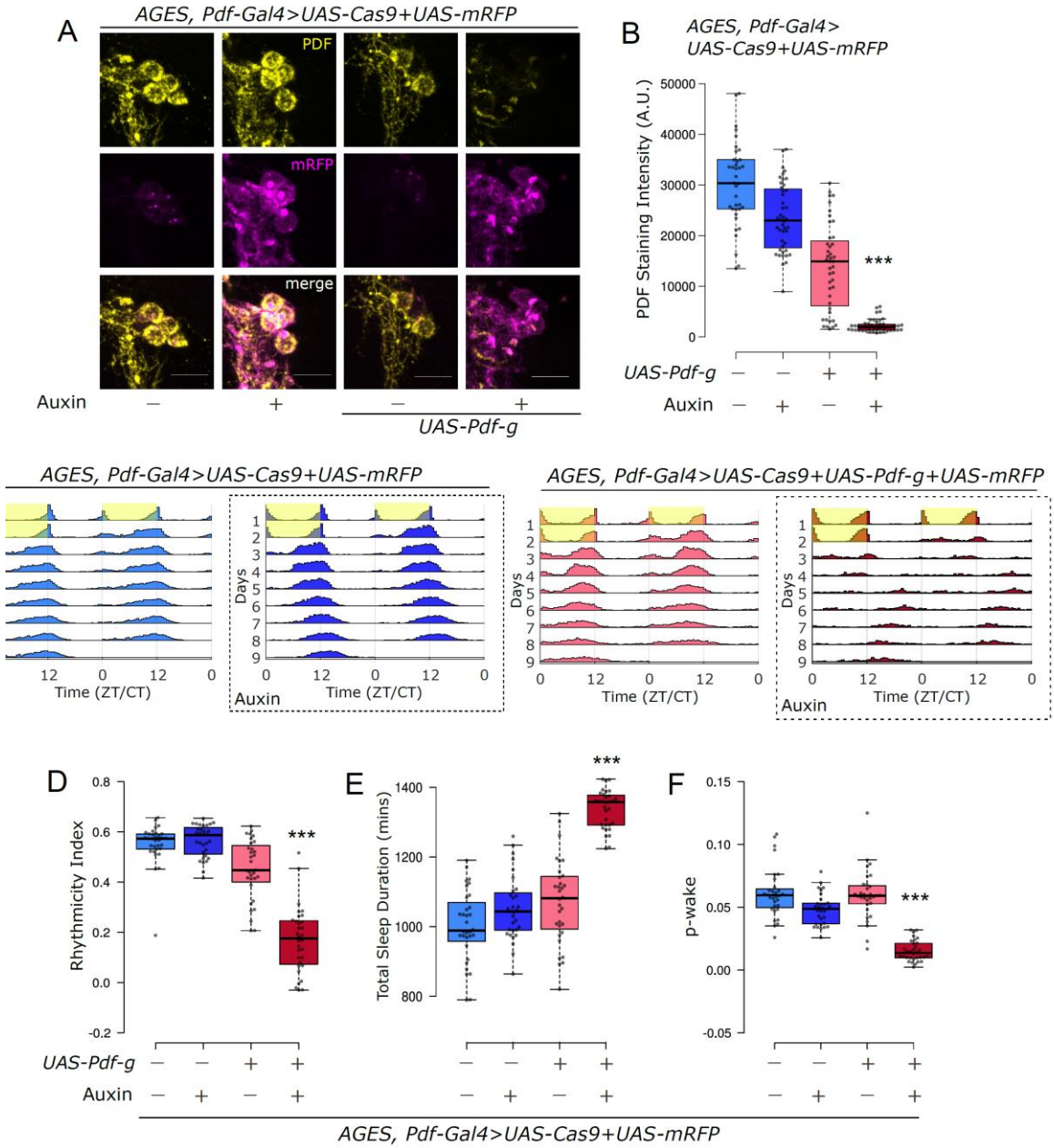

Fig. 5: Adult-specific loss of PDF with AGES leads to loss of rhythmicity and wakefulness. **A**. Representative images of sLNvs stained for mRFP and PDF. Upon feeding 10mM auxin for 2 weeks, there is loss of PDF staining in cells expressing both *UAS-Cas9* and *UAS-Pdf-g*. Scale bar represents 10µm. **B**. Quantification of PDF staining intensity from sLNvs is represented with boxplots, n ≥ 39 cells from at least 11 hemibrains per genotype/condition. There is a significant effect of both variables on PDF staining intensity and a significant interaction when AGES and CRISPR reagents for *Pdf* were combined with auxin feeding (Two-way ANOVA; *** Interaction

p<0.001). **C**. Actograms represent double-plotted average activity of flies from an experiment across multiple days. Yellow panels indicate lights ON. Panels in dotted boxes indicate auxin feeding. **D**. Rhythmicity Index for individual flies quantified (from DD2-7) represented by a boxplot, n ≥ 31 per genotype. There is a significant effect of both variables on rhythmicity and a significant interaction when AGES and CRISPR reagents for *Pdf* were combined with auxin feeding (Two-way ANOVA; *** Interaction p<0.001). **E**. Total sleep duration in a day for individual flies quantified (from DD1-4) represented by a boxplot. There is a significant effect of both variables on sleep duration and a significant interaction when AGES and CRISPR reagents for *Pdf* were combined with auxin feeding (Two-way ANOVA; *** Interaction p<0.001). **F**. p-wake over a 24-hour period for individual flies quantified (from DD1-4) represented by a boxplot. There is a significant effect of both variables on p-wake and a significant interaction when AGES and CRISPR reagents for *Pdf* were combined with auxin feeding (Two-way ANOVA; *** Interaction p<0.001).

Genotype	Cells labelled	n	Rhythmicity Index LL2-7 (Mean ± SEM)	%Rhythmic	Period (h) (Mean ± SEM)
CLK856-Gal4>UAS-Cas9	Most clock neurons (many DN3s missing)	85	0.13 ± 0.01	10.6	-
CLK856-Gal4>UAS-cry-g		72	0.11 ± 0.01	6.9	-
CLK856-Gal4>UAS-Cas9+UAS-cry-g		**92**	**0.40 ± 0.01**	**90.2**	**24.71 ± 0.07**
PDF-Gal4>UAS-Cas9	sLNvs+ lLNvs	118	0.10 ± 0.01	6.8	-
PDF-Gal4>UAS-cry-g		119	0.12 ± 0.01	5.0	-
PDF-Gal4>UAS-Cas9+UAS-cry-g		**121**	**0.17 ± 0.01**	**14.9**	-
dvPDF-Gal4>UAS-Cas9	sLNvs+ lLNvs+ 5th sLNv+ 1 CRY^{+} ITP^{+} LNd + 3 CRY^{-}LNds	56	0.14 ± 0.01	8.9	-
dvPDF-Gal4>UAS-cry-g		51	0.15 ± 0.01	9.8	-
dvPDF-Gal4>UAS-Cas9+UAS-cry-g		**58**	**0.52 ± 0.02**	**91.4**	**24.24 ± 0.06**
MB122B-Gal4>UAS-Cas9	5th sLNv + 1 CRY^{+}ITP^{+} + 2 CRY^{+} Trissin^{+} LNds	64	0.15 ± 0.01	9.4	-
MB122B--Gal4>UAS-cry-g		61	0.14 ± 0.01	3.3	-
MB122B-Gal4>UAS-Cas9+UAS-cry-g		**63**	**0.37 ± 0.02**	**79.4**	**25.08 ± 0.08**
ss00639-Gal4>UAS-Cas9	5th sLNv + 1 CRY^{+}ITP^{+} LNd	64	0.14 ± 0.01	9.4	-
ss00639-Gal4>UAS-cry-g		58	0.15 ± 0.01	10.3	-
ss00639-Gal4>UAS-Cas9+UAS-cry-g		**60**	**0.41 ± 0.01**	**91.7**	**25.11 ± 0.06**
ss00773-Gal4>UAS-Cas9	5th sLNv + 1 CRY^{+}ITP^{+} LNd	63	0.14 ± 0.01	4.8	-
ss00773-Gal4>UAS-cry-g		60	0.15 ± 0.01	8.3	-
ss00773-Gal4>UAS-Cas9+UAS-cry-g		**61**	**0.29 ± 0.02**	**60.7**	**25.06 ± 0.14**
CLK4.1-Gal4>UAS-Cas9	DN1p	72	0.12 ± 0.01	9.7	-
CLK4.1-Gal4>UAS-cry-g		69	0.13 ± 0.01	5.8	-
CLK4.1-Gal4>UAS-Cas9+UAS-cry-g		**83**	**0.33 ± 0.01**	**74.7**	**21.82 ± 0.08**

Table 1: Summary of circadian behavior with cell type-specific CRY mutants in constant light.

Genotype	cells labelled	n	Percent Rhythmic	Rhythmicity Index (DD1-4)	Average total sleep per day (min)	Activity while awake	pwake	pdoze
PDF-Gal4>UAS-Cas9	All sLNVs +lLNVs	63	98.4	0.37 ± 0.01	914 ± 22	1.62 ± 0.04	0.12 ± 0.01	0.37 ± 0.01
PDF-Gal4>UAS-PDFg		62	90.3	0.33 ± 0.01	873 ± 23	1.79 ± 0.05	0.13 ± 0.01	0.35 ± 0.01
PDF-Gal4>UAS-Cas9 + UAS-PDFg		61	24.6	**0.14 ± 0.01**	**1178 ± 19**	**2.52 ± 0.10**	**0.06 ± 0.00**	0.40 ± 0.01
ss00681-Gal4>UAS-Cas9	All sLNVs	63	96.8	0.36 ± 0.01	924 ± 19	1.81 ± 0.04	0.12 ± 0.01	0.38 ± 0.01
ss00681-Gal4>UAS-PDFg		62	83.9	0.29 ± 0.01	972 ± 21	2.17 ± 0.07	0.12 ± 0.01	0.42 ± 0.01
ss00681-Gal4>UAS-Cas9 + UAS-PDFg		55	23.6	**0.13 ± 0.01**	**1284 ± 13**	**2.57 ± 0.10**	**0.04 ± 0.00**	0.44 ± 0.01
ss00645-Gal4>UAS-Cas9	variably 2-4 lLNVs per hemisphere	62	96.8	0.39 ± 0.01	957 ± 23	1.79 ± 0.05	0.11 ± 0.01	0.34 ± 0.01
ss00645-Gal4>UAS-PDFg		61	96.7	0.32 ± 0.01	1068 ± 14	2.37 ± 0.10	0.08 ± 0.00	0.38 ± 0.01
ss00645-Gal4>UAS-Cas9 + UAS-PDFg		63	95.2	0.35 ± 0.01	**1142 ± 15**	2.20 ± 0.08	**0.07 ± 0.00**	0.38 ± 0.1

Table 2: Summary of circadian and sleep behavior upon loss of PDF from specific neurons.

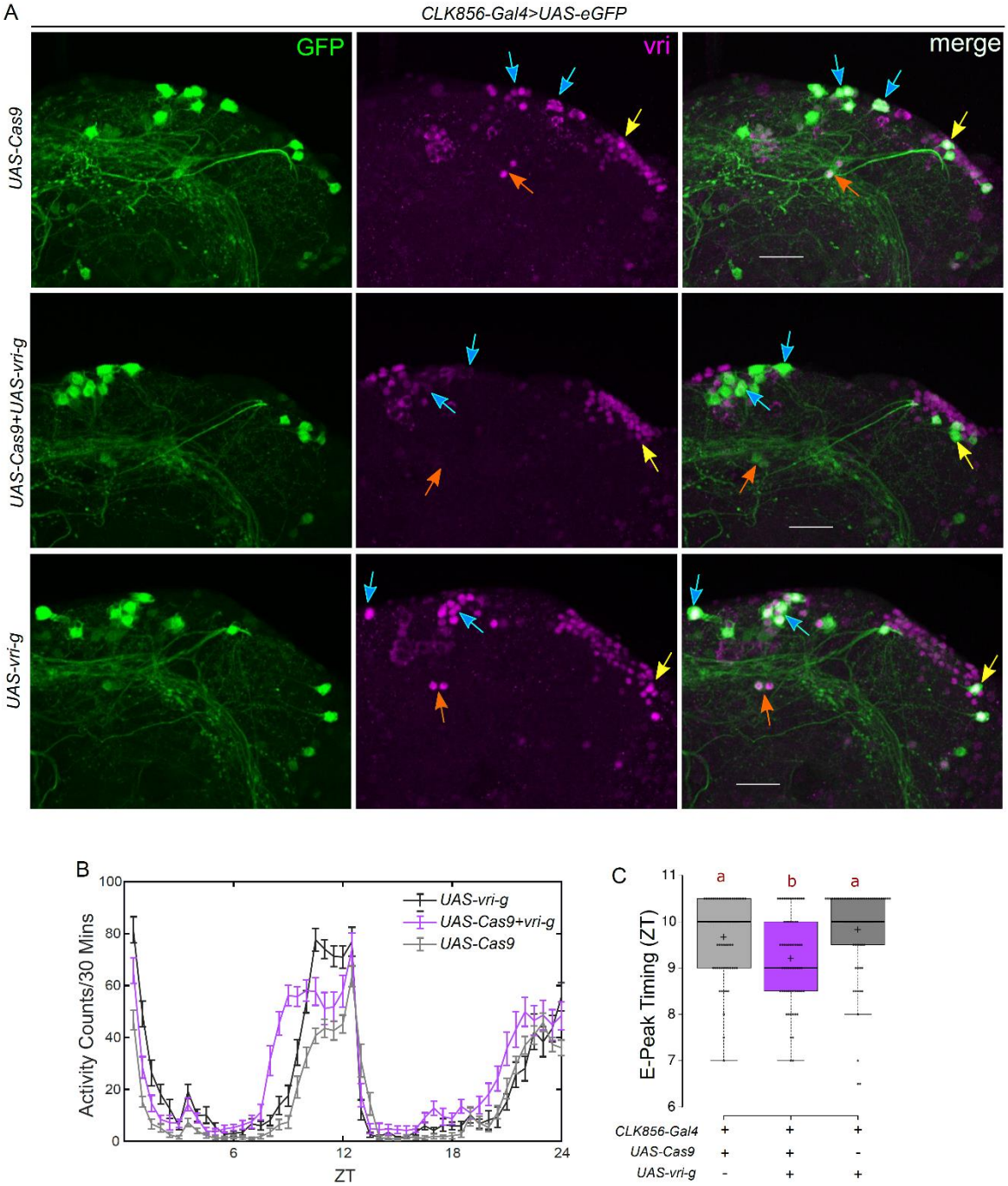

Fig. S1: Loss of VRI from clock neurons leads to an advanced evening peak. A. Representative images of the dorsal circadian neurons stained for GFP and VRI at ZT19. There is loss of VRI staining in cells expressing *CLK856-Gal4* (marked by GFP) but no loss in GFP-negative cells.

Arrows point to examples of Gal4-positive DN1s (blue), DN2s (red) and DN3s (yellow) in the indicated genotypes. Scale bar represents 20µm. **B**. Average activity counts for flies in an experiment plotted as a function of time. Flies with loss of VRI in *CLK856-Gal4* labelled neurons showed an advanced evening peak. **C**. Quantification of the evening peak (E-peak) timing from individual flies, $n \geq 62$ per genotype from at least two independent experiments. Letters represent statistically distinct groups; $p<0.01$, Kruskal Wallis test followed by a post hoc Dunn's test.

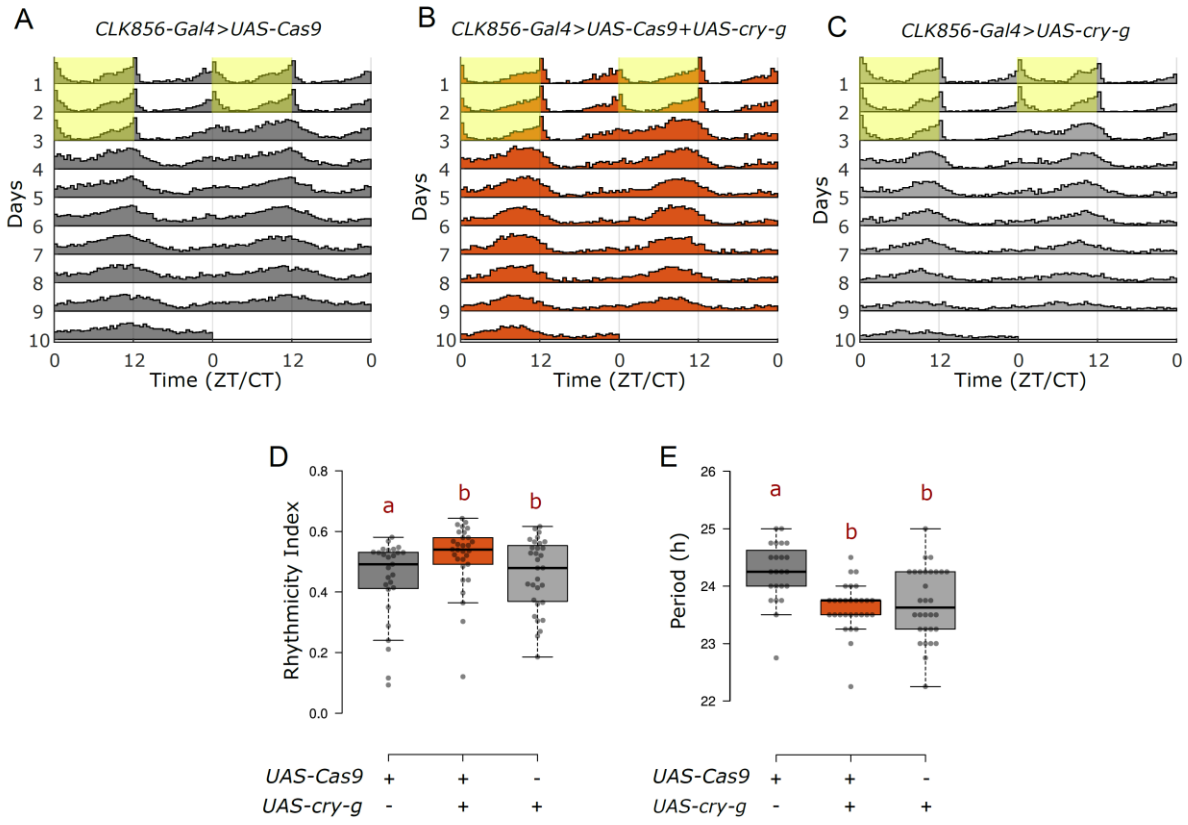

Fig. S2: CRY mutation in clock neurons does not affect circadian behavior under constant darkness. A-C. Actograms represent double-plotted average activity of flies from an experiment across multiple days. Yellow panels indicate lights ON. **D**. Rhythmicity Index for individual flies quantified for DD2-7 represented by a boxplot, n ≥ 27 per genotype, letters represent statistically distinct groups, p<0.01, Mann-Whitney U test post Kruskal Wallis ANOVA. **E**. Free running period under constant darkness for individual flies quantified for DD2-7 represented by a boxplot, letters represent statistically distinct groups; p<0.01, Kruskal Wallis test followed by a post hoc Dunn's test.

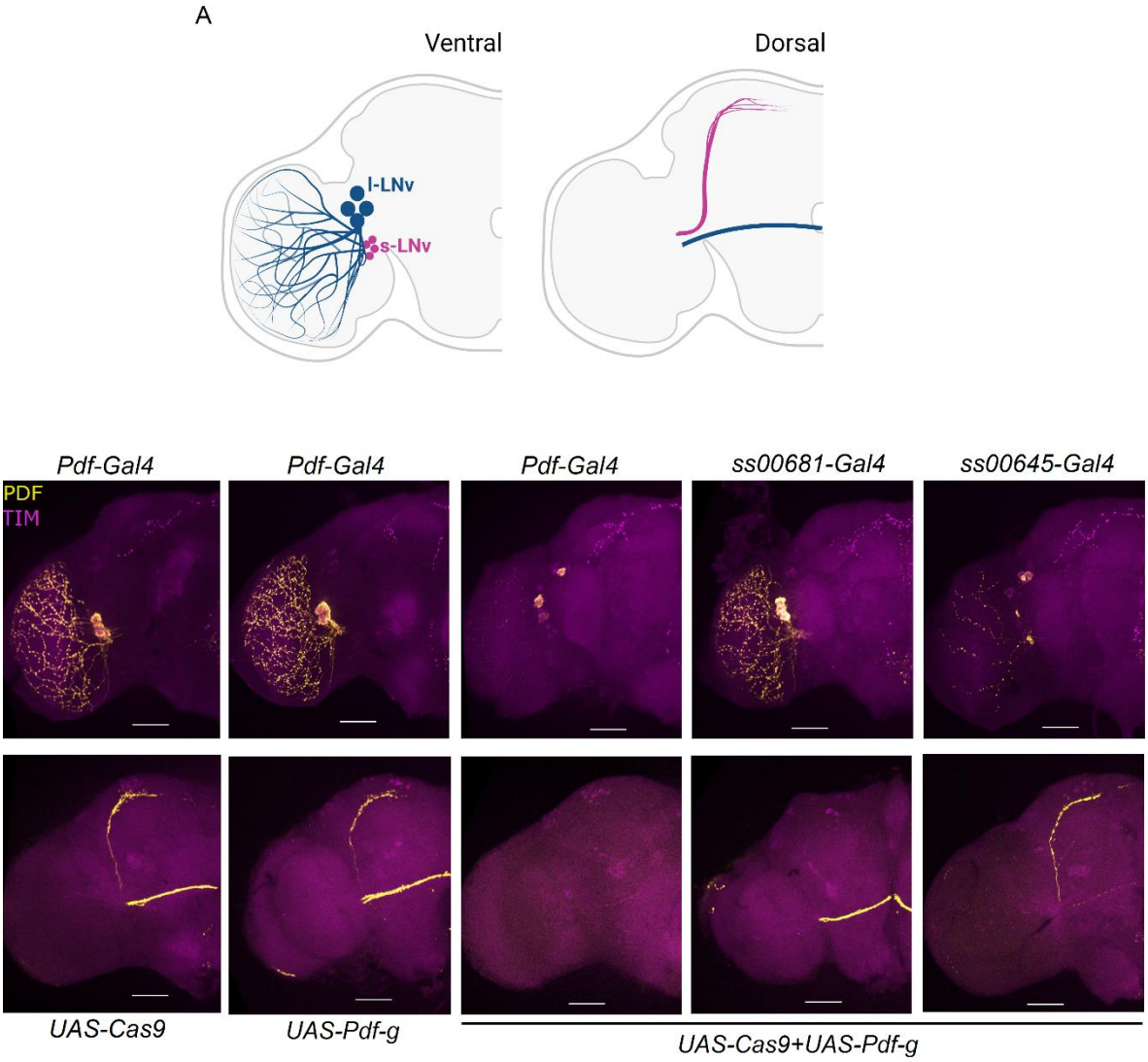

Fig. S3: CRISPR strategy successfully eliminates PDF staining from cell type-specific projections. A. Cartoon representation of the projection patterns of small (magenta) and large (blue) LNV neurons in the ventral and dorsal *Drosophila* brain. **B**. Representative images of hemibrains imaged from the ventral (top) or dorsal (bottom) side stained for PDF and TIM. For the dorsal panels, brightness-contrast was enhanced for the PDF channel equally across genotypes to confirm absence of PDF staining from the respective processes. Expression of both *UAS-Cas9* and *UAS-Pdf-g* with *Pdf-Gal4* leads to loss of all PDF staining from all PDF neurons. Expression with *ss00681-Gal4* that labels only the sLNvs leads to loss of PDF staining from their cell bodies and projections with no obvious effect on PDF staining in lLNvs. Expression with *ss00645-Gal4* leads to loss of PDF staining in most projections of these neurons with no obvious effect on PDF staining in sLNvs.

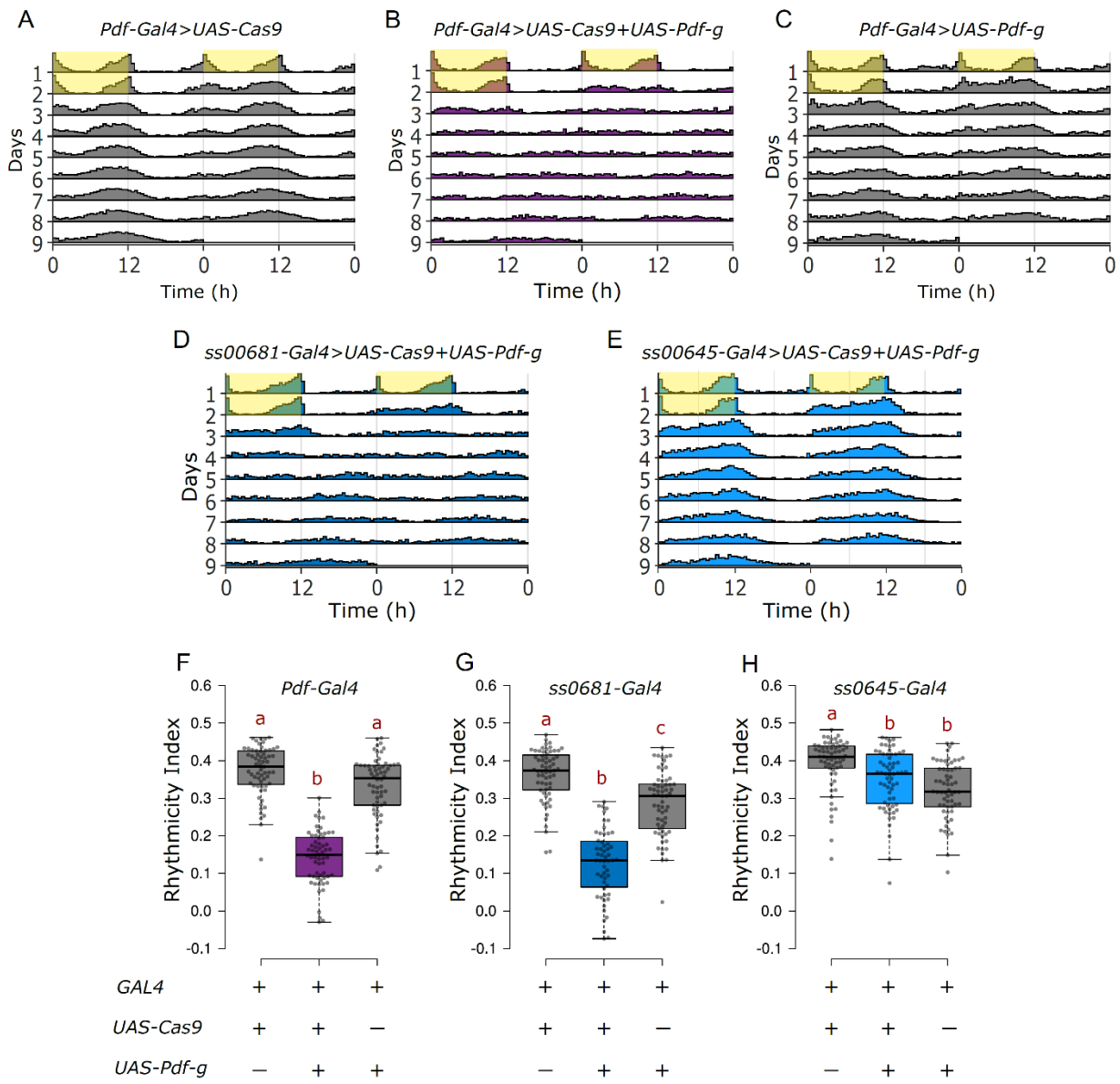

Fig. S4: Loss of PDF from sLNvs leads to loss of rhythmicity under constant darkness. A-E. Actograms represent double-plotted average activity of flies from an experiment across multiple days. Yellow panels indicate lights ON. **F-H**. Rhythmicity Index for individual flies quantified for DD1-4 represented by a boxplot, n ≥ 55 per genotype from at least two independent experiments, letters represent statistically distinct groups; p<0.01, Kruskal Wallis test followed by a post hoc Dunn's test. Loss of PDF from both sLNvs and lLNvs or from sLNvs alone causes arrhythmicity in constant darkness, whereas loss of PDF from lLNvs alone has no effect.

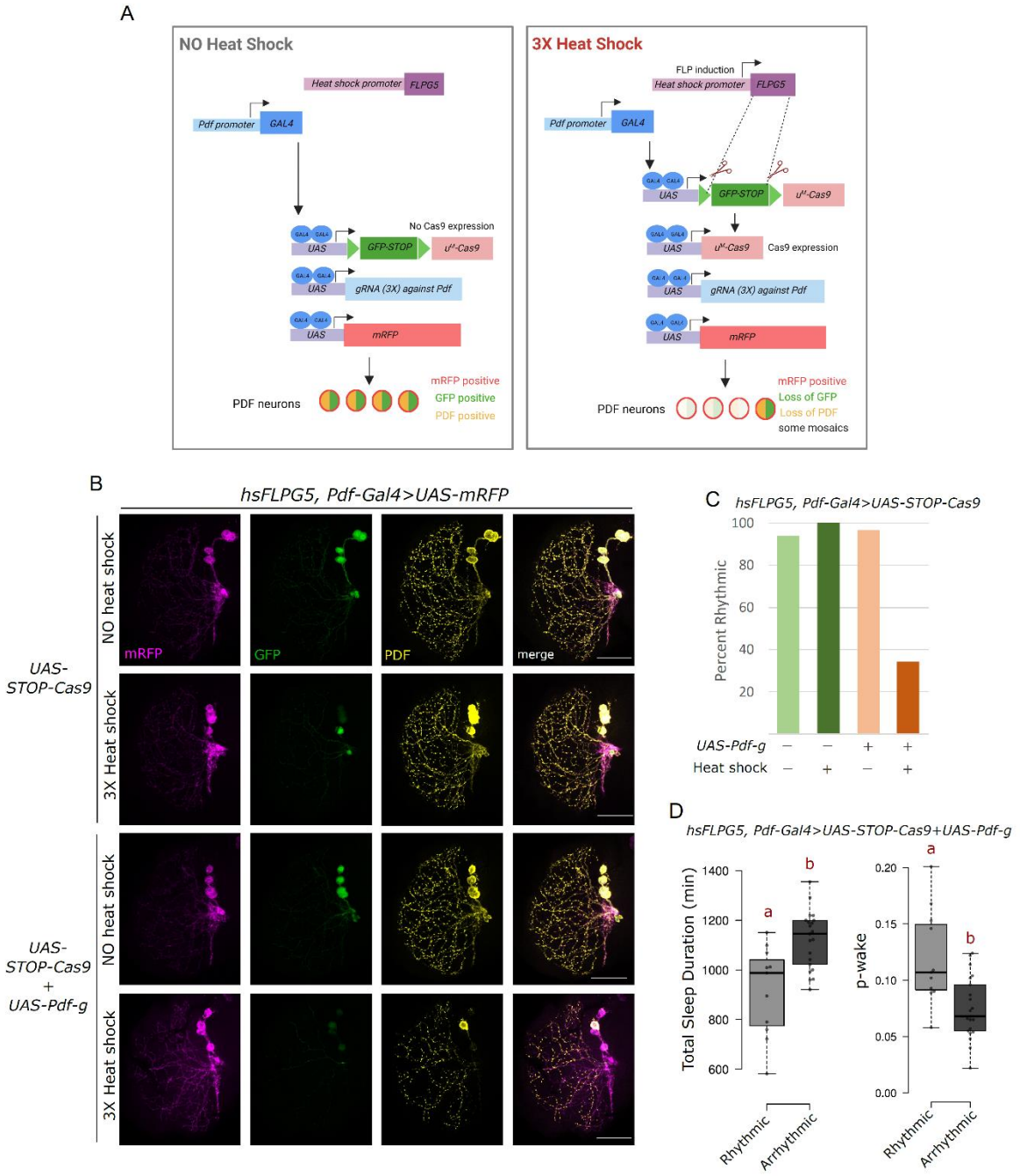

Fig. S5: The inducible-Cas9 systems is an effective tool for adult specific and cell type specific CRISPR mutagenesis despite some mosaics. A. Cartoon representation of the inducible Cas9 system (Port et. al., 2020) adapted to the adult-specific perturbation of PDF from PDF neurons. **B**. Representative images of the optic lobe ventral projections of the lLNvs. Scale bar represents 50µm. **C**. Plot indicating the percentage of flies rhythmic under the indicated conditions. **D**. Sleep parameters of flies expressing both *UAS-Cas9* and *UAS-Pdf-g* with heat-shock separated

into rhythmic (RI>0.25) and arrhythmic (RI<0.25) categories, n=11 for rhythmic and 21 for arrhythmic. Arrhythmic flies have more sleep and a lower p-wake; $p<0.01$, Mann Whitney U test. These rhythmic flies could be the result of the mosaicism, i.e., PDF expression in 1-2 sLNvs might be sufficient for quasi-normal circadian and sleep behavior.

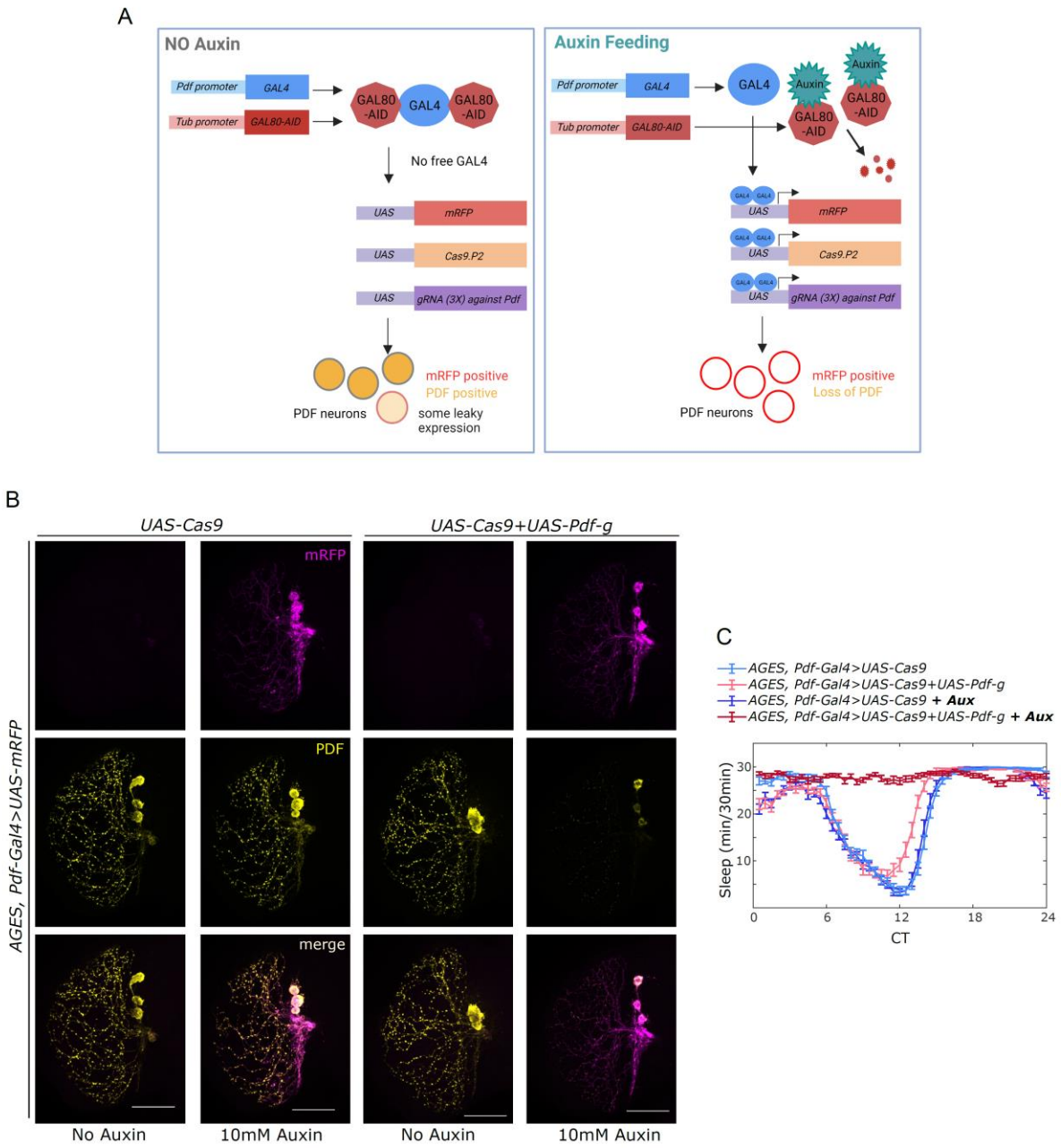

Fig. S6: AGES is mildly leaky, but still an effective tool for adult-specific, cell type-specific CRISPR mutagenesis. A. Cartoon representation of the AGES system (McClure et. al., 2022) adapted to the adult specific perturbation of PDF from PDF neurons. **B**. Representative images of the optic lobe ventral projections of the lLNvs. Scale bar represents 50µm. **C**. Sleep plot representing average sleep of flies from DD1-4 in 30-minute bins.

Genotype	Reference/Source	Stock number
CLK856-Gal4	(Gummadova et al., 2009); Bloomington Drosophila Stock Center	BDSC 93198
UAS-eGFP	Bloomington Drosophila Stock Center	BDSC 5430
UAS-mRFP	Bloomington Drosophila Stock Center	BDSC 32219
UAS-Cas9.P2 (attP40)	Bloomington Drosophila Stock Center	BDSC 58985
AGES	(McClure et al., 2022); Bloomington Drosophila Stock Center	BDSC 92470
hsFLPG5	Bloomington Drosophila Stock Center	BDSC 55814
PDF-Gal4	(Renn et al., 1999)	NA
CLK4.1-Gal4	(Zhang et al., 2010)	NA
dvPDF-Gal4	(Bahn et al., 2009)	NA
MB122B-Gal4	(Guo et al., 2017)	H Dione, A Nern and G Rubin, (Janelia Research Campus)
ss00681-Gal4	(Liang et al., 2017)	
ss00645-Gal4	(Schlichting et al., 2019)	
ss00639-Gal4	Le et. al., In prep	
ss00773-Gal4	Le et. al., In prep	
UAS-STOP-Cas9 (UAS-FRT-mEGFP-FRT-uM-Cas9)	(Port et al., 2020); Vienna Drosophila Resource Center	VDRC 340008
UAS-3X-vrig (attP2)	This study	NA
UAS-3X-cryg (attP2)	This study	NA
UAS-3X-Pdfg (attP2)	This study	NA

Table S1: List of fly strains.

name	sequence 5'-> 3'
vri-1	GGCCCGGGTTCGATTCCCGGCCGATGCA**TACAGCCAGCAGAAGCTGAG**GTTTCAGAGCTATGCTGGAAAC
vri-2	**ACTGCGGTCCATTGCCACCC**TGCACCAGCCGGGAATCGAACC
vri-3	**GGGTGGCAATGGACCGCAGT**GTTTCAGAGCTATGCTGGAAAC
vri-4	TTTAACTTGCTATTTCTAGCTCTAAAAC**GACATTGCGGTTTAGTGCCT**TGCACCAGCCGGGAATCGAACC
cry-1	GGCCCGGGTTCGATTCCCGGCCGATGCA**CGCGAGGGGCGAATGTGATT**GTTTCAGAGCTATGCTGGAAAC
cry-2	**CCTGTAGCTGATCATCGATG**TGCACCAGCCGGGAATCGAACC
cry-3	**CATCGATGATCAGCTACAGG**GTTTCAGAGCTATGCTGGAAAC
cry-4	TTTAACTTGCTATTTCTAGCTCTAAAAC**TACACATTGAAGTGCTCCGG**TGCACCAGCCGGGAATCGAACC
Pdf-1	GGCCCGGGTTCGATTCCCGGCCGATGCA**TGCTGCCAGTGGGGATACTG**GTTTCAGAGCTATGCTGGAAAC
Pdf-2	**CGTTGTTGAACCAGTCGAGG**TGCACCAGCCGGGAATCGAACC
Pdf-3	**CCTCGACTGGTTCAACAACG**GTTTCAGAGCTATGCTGGAAAC
Pdf-4	TTTAACTTGCTATTTCTAGCTCTAAAAC**GCATCGTTCATGTTCTTGGG**TGCACCAGCCGGGAATCGAACC

Table S2: List of primers.